GCA TECHNICAL REPORT NO. 66-3-N

DEVELOPMENT OF A MASS SPECTROMETER EMPLOYING A PHOTOIONIZATION SOURCE

W. P. POSCHENRIEDER

A. F. BARRINGTON

GCA CORPORATION

Bedford, Massachusetts

FINAL REPORT

CONTRACT NO. NAS1-4927

PREPARED FOR

NATIONAL AERONAUTICS AND SPACE ADMINISTRATION

LANGLEY RESEARCH CENTER

HAMPTON, VIRGINIA

FEBRUARY 1966

GCA Technical Report 66-3-N

DEVELOPMENT OF A MASS SPECTROMETER EMPLOYING A PHOTOIONIZATION SOURCE

W.P. Poschenrieder A.F. Barrington

FINAL REPORT

Contract No. NAS1-4927

February 1966

GCA CORPORATION
GCA TECHNOLOGY DIVISION
Bedford, Massachusetts

Prepared for

NATIONAL AERONAUTICS AND SPACE ADMINISTRATION
Langley Research Center
Hampton, Virginia

TABLE OF CONTENTS

LIST OF ILLUSTRATIONS

LIST OF ILLUSTRATIONS (continued)

DEVELOPMENT OF A MASS SPECTROMETER EMPLOYING A PHOTOIONIZATION SOURCE

By W. P. Poschenrieder and A. E. Barrington
GCA Corporation, GCA Technology Division
Bedford, Massachusetts

SUMMARY

The present report deals with the construction of a mass spectrometer that uses photoionization for the ion production. By the use of uv light and in particular with a uv vacuum monochromator to select the proper wavelength, simplified spectra generally are achieved, since in contrast to the commonly used electron impact ion source fragmentation of molecules can be suppressed. Additional advantages are the exclusion of chemical reactions with hot filaments and the elimination of outgassing from heated elements that are present in electron impact ion sources.

Beyond these general advantages, the method offers a unique possibility to differentiate gases which peak at the same mass number, such as N_2 and CO. This is possible because the ionization potential of these gases is different. This method also affords the possibility of selecting the energy of the ionizing photons with a precision yet unsurpassed by any other method of ionization. These results can only be equaled by high resolution mass spectrometry, although this involves considerably more complex equipment and complex methods for the interpretation of the spectra.

The work performed under the contract clearly shows the advantages a photoionization mass spectrometer offers over conventional instruments, in particular when weight and simplicity of equipment and spectra are important factors. These demands are mandatory in space missions, and a mass spectrometer of this new type seems to be the most feasible way for monitoring the atmosphere in a space capsule, especially the build-up of toxic gases.

The equipment described in the report was built strictly as a ground laboratory instrument without specific regard to weight or power consumption. It was, therefore, designed to achieve the utmost in sensitivity, accuracy, and reliability in order to evaluate the more basic limits of our method. The result is an instrument which also allows a more general application to a number of modern fields of investigation.

The data produced show the very fine performance of the mass spectrometer and also give very promising results for the differentiation between CH_4 and O and between CO and N_2. The results also reveal the limitations presently encountered and their source which solely lies in the monochromator, which is a commercial type owned by GCA Corporation. At present, 100 ppm of CH_4 in a pure O_2 atmosphere and 0.5 percent of CO in an N_2 atmosphere can be detected. It is thought, however, that some alterations of the monochromator will extensively improve the detection of CO in N_2.

INTRODUCTION

Mass spectroscopy under ideal conditions is a powerful analytical tool and is capable of detecting trace impurities in concentrations as small as 1 part in 10^9 [1].* When applied to the analysis of a space capsule atmosphere, however, the following limitations of a conventional instrument arise:

(1) Ionization by electron impact in the ion source causes dissociation, fragmentation, and multiple ionization of gas molecules all of which result in a characteristic spectral pattern for a given substance. In consequence, direct identification of a gas mixture is possible in only the most elementary cases. A more complicated spectrum of a space capsule for instance, can be interpreted - if at all - only after solving a more or less complex set of simultaneous equations derived from mass spectrometer records.

(2) Because of the hot filament and the accordingly increased operating temperature of the ion source, thermal decomposition and pyrolysis occur as does outgassing from the filament and from the hot parts of the ion source. All these effects contribute to mass peaks, such as NO, CO, and H_2, which are extraneous to the real atmosphere under investigation. Differential pumping between the filament region and the ionization chamber improves this situation but also reduces the sensitivity.

(3) The extremely small separation on the atomic mass scale of certain important mass peaks requires an instrument of high resolving power, necessitating large, heavy, and very complex equipment. However, because of the close proximity of such peaks, the sensitivity is related to the relative magnitude of the peaks and is limited if the disparity is large.

*Numbers in [ ] represent reference numbers.

It is important to note the real meaning of the so-called "sensitivity" for trace impurities, as referred to in many advertisements. It implies that one part of a trace impurity added to one million parts of a gas sample results in a mass peak just detectable above the noise level. However, this is the case only when the trace peak has a position which is completely free of any background due to the spectrum of the pure gas sample. This very important condition is normally omitted in the advertisements. Actually, the background of a clean air sample covers most mass numbers in the lower half of the mass range and some in the upper, and is many orders of magnitude larger than the claimed sensitivity of one part per million. Accordingly, the actual sensitivity is limited. Because of the fragmentation of molecules by electron impact and the presence of the naturally occurring isotopes of the component elements of normal atmospheric gases, most of the mass numbers of known toxic gases up to 34 are already occupied by the more intense peaks of the regular air spectrum.

For demonstration, let us disregard the usual background gas contamination from the ion source and mass spectrometer and consider the regular mass spectrum of clean air as obtained with an ideal electron impact ion source (see Table 1).

The intensity figures have been calculated in parts per million using the normal composition of air and the normal isotope ratios under the simplifying assumption of equal ionization probability. The fragment ions H, HH, and HO from HHO; C from COO; N from NN; and O from OO have been assumed to have half the intensity of the parent peak. From this table, it is seen that half the mass numbers below mass 44 are occupied by regular air peaks which are far above the desired detection limit of one part per million.

Let us now compare this air background list with the following list of known toxic gases of low mass numbers [2,3]:

	Mass Number	Toxicity Level PPM
Ammonia NH_3	17	100
Hydrogen Fluoride HF	20	3
Hydrogen Cyanide HCN	27	20
Carbon Monoxide CO	28	100
Formaldehyde CH_2O	30	10
Nitric Oxide NO	30	25
Fluorine F_2	38	1
Carbon Dioxide CO_2	44	> 5000
Ozone	48	> 0.1 per eight hour day

TABLE 1

COMPOSITION OF AIR

Molecule	Mass Number	Relative Concentration (ppm)
H	1	> 5000
HH	2	> 5000
C^{12}	12	>> 150
N^{14}	14	390,000
N^{15}	15	1400
O^{16}	16	100,000
HO^{16}	17	5,000
$HH\ O^{16} + HO^{17} + DO^{16}$	18	10,000
$HH\ O^{17} + HO^{18} + HD\ O^{16}$	19	1,400
$HH\ O^{18} + Ne^{20}$	20	40
$N^{14}N^{14}$	28	780,000
$N^{14}N^{15}$	29	6,200
$N^{15}N^{15}$	30	>> 13
$O^{16}O^{16}$	32	210,000
$O^{16}O^{17}$	33	155
$O^{16}\ O^{18} + O^{17}\ O^{17}$	34	860
Ar^{36}	36	32
Ar^{38}	38	6
Ar^{40}	40	9,400
$C^{12}\ O^{16}\ O^{16}$	44	> 300

The toxicity level given in here is the maximum acceptable amount per eight hour day and repeated exposure for an indefinite period of days.

One sees that most of these mass numbers of the toxic gases are already occupied by more intense peaks of the regular air spectrum. This is not only true for the parent peaks but also for all fragment ions. The HCN peak at mass 27 is the only one that does not coincide with an air peak. However, it is adjacent to the biggest peak, N_2 at mass 28, and may be obscured by the tail of this peak. This means that these toxic gases cannot be detected in air with any simple electron impact type mass spectrometer even if the instrument is more sensitive than one part per million. It would not be too difficult to detect such toxic gases at a one part per million level in hydrogen because there would be no interference with any background peaks. The root of the difficulty lies in the requirement that the toxic gases should be detected in regular air.

The foregoing discussion leads to the following conclusions:

(1) It is not possible to build a flyable conventional mass spectrometer that can detect small concentrations of light toxic gases (below mass 34) in air.

(2) Only a very large laboratory instrument, especially designed for this purpose, is capable of this difficult analysis. It would be very useful for the analysis of air in a space capsule during a ground experiment. However, the operation of such an instrument and the data interpretation are difficult and require an experienced mass spectroscopist.

A Photoionization Mass Spectrometer offers considerable advantages toward a solution to the problem. Since the ion source works at room temperature, outgassing and pyrolysis are omitted. The absence of a hot filament also permits running the ion source at pressures up to 20μ, even with pure O_2. Thus the contribution of residual gases at a background pressure of 2×10^{-7} in the mass spectrometer is 5 orders of magnitude below the air sample. Accordingly, CO from the natural background gas is well below 10 parts in 10^6 of the atmosphere to be controlled.

The total superiority of photoionization for gas analysis is realized if the mass spectrometer is combined with a uv monochromator. This allows setting of the ionizing photon energy with an accuracy of 0.02 eV at an energy of about 16 eV.

TABLE 2

IONIZATION POTENTIALS OF VARIOUS GASES

Mass Number	Gas	Ionization Potential	Wave-length Å
16	CH_4	12.98	955
17	NH_3	10.15	1220
18	H_2O^{16}	12.59	985
	H_2O^{17}, HDO^{16}	12.59	985
20	HF	15.77	785
	H_2O^{18}, DDO^{16}	12.59	985
27	HCN	13.91	890
28	CO	14.01	885
	N_2^{14}	15.58	795
29	$N^{14}N^{15}$	15.58	795
30	CH_2O	10.87	1140
	N_2^{15}	15.58	795
	$N^{14}O^{16}$	9.25	1340
32	O_2^{16}	12.07	1027
33	$O^{16}O^{17}$	12.07	1027

TABLE 2 (Cont.)

Mass Number	Gas	Ionization Potential	Wave-length Å
34	$O^{16}O^{18} + O_2^{17}$	12.07	1027
	H_2S	10.46	1185
36	Ar^{36}	15.75	786
38	F_2	15.7	790
40	Ar^{40}	15.75	786
44	CO_2	13.79	899
48	O_3	12.8	968

The advantage of this arrangement is apparent when the ionization potentials and corresponding wavelengths of the toxic gases of mass numbers up to 48 are compared (Table 2) with those of the atmospheric gases occupying the same or adjacent mass peaks.

In this list, we have already omitted all fragment ions given in the first list. The corresponding threshold energies for these ions are usually much higher. None of them will appear if the ionization energy is set below 16 eV. This energy, however, is sufficient to ionize any of the toxic gases in this range.

In detail the photoionization method offers the following advantages over electron impact:

(1) Since the threshold energy for an OH-ion out of H_2O is 18.5 eV, any lower energy down to 10.15 eV will only produce NH_3^+ at mass 17.

(2) The ionizing potentials of HCN (mass 27) and the predominant $N^{14}N^{14}$ (mass 28) are sufficiently well separated to make it possible to ionize HCN without ionizing $N^{14}N^{14}$.

(3) The ionizing potentials of CO and $N^{14}N^{14}$ (mass 28) are sufficiently far apart to ionize CO without ionizing $N^{14}N^{14}$.

(4) The ionizing potentials of the gases at mass 30 are sufficiently far apart to enable the separation of CH_2O, $N^{14}O^{16}$ and $N^{15}N^{15}$.

(5) In the case of HF (mass 20) the ionizing potential is so high that the normal atmospheric gases occupying these peaks are more easily ionized. Thus the detection limit is 40 ppm according to Table 1.

(6) F_2 and ^{38}A show only a very small difference in the ionization potential. However, the concentration of ^{38}A in air amounts to 6 ppm and little discrimination power is required to detect 1 ppm of F_2.

In the mass range 50 to 100 where spectral peaks of organic compounds are to be expected, photoionization also considerably reduces the degree of fragmentation; here, the ease of accurate selection of the wavelength by means of a monochromator would greatly simplify the interpretation of hydrocarbon spectra. A considerable amount of information regarding ionization cross sections and fragmentation of hydrocarbon vapors by photoionization is now available [4,5,6] and will facilitate the detection of such substances.

The only drawback of the photoionization mass spectrometer compared with electron impact type instruments is the lower ion current. Consequently, high sensitivity is problematic. The reason is, that to date, copious amounts of electrons are generated more easily than high photon fluxes. Hurzeler et al.[7] quote maximum ion currents of 10^{-15}A; Dibeler and Reese [8] obtained only 10^{-17}A. If these were the optimum achievable ion currents, the prospects of utilizing the photoionization mass spectrometer for sensitive gas analysis would be indeed dim. Fortunately, the situation can be improved by a careful design of the apparatus.

By use of a low pressure uv spark source, light intensities of the order of 10^9 photons/sec can be attained at the exit slit of a monochromator provided strong emission lines are selected. If 10 percent of this intensity could be utilized for ion production, with an ionization efficiency of about 50 percent, and if further, an ion collection efficiency of 10 percent is assumed, the resulting ion current is 8×10^{-13}A. This is one hundred times more than quoted by Hurzeler et al. [7]. However, this estimated improvement can be realized only with ion source pressures high enough to insure the absorption of an appreciable fraction of the available light intensity; in addition, the ion collection efficiency must be favorable. Most of the previous investigators worked with ion source pressures in the 10^{-4} mm Hg range corresponding to less than 0.1 percent light absorption. They mostly used analyzers of the 60 degree sector field type which are characterized by a small solid angle collection efficiency and a correspondingly low factor of transmission. Comes and Lessman [9] employed a quadrupole mass analyzer, but similarly were forced to work with wide apertures at the expense of resolution to obtain desirable ion intensities.

The omission of a dispersing device for the uv would yield a strong increase in the available ion current; this, however, would result in less versatility. In this case, resonance light sources are the best because they provide nearly monochromatic radiation. The available intensities can be judged from measurements by Jensen and Libby [10] on a helium light source to be of the order of 10^{15} photon/cm^2, or 5×10^{12} photons/sec when a slit of 5 mm high and 0.1 mm wide is used, which is equivalent to the slit used on the monochromator. However, only three resonance light sources are available for use in the photoionization spectral region: helium, neon, and argon. Only helium and neon will ionize most of the common gases. The neon source is more favorable with respect to fragmentation than helium, but even the helium source produces less fragmentation than electron impact ionization. Although undispersed radiation will yield a gain in intensity of three orders of magnitude, the inability to work near the threshold of ionization or to discriminate between two ions of the same mass diminishes the advantages of a photoionization mass spectrometer.

The following sections describe the design and performance of a photoionization mass spectrometer which was designed to overcome some of the problems mentioned here and which allows evaluation of the limits of the present state of the art.

INSTRUMENT DESIGN

The intention was to build a versatile laboratory instrument without regard to the requirements of a flyable instrument as far as weight, dimensions, and power consumption are concerned. This resulted in an instrument which safely allows the evaluation of the capabilities of the method and establishes its practical limits. The feasibility of a flyable version of the present instrument is discussed in the Appendix.

Figure 1 shows the basic arrangement. The light beam from the spark source enters the monochromator through the externally adjustable entrance slit. The light is dispersed on the concave grating which produces a monochromatic image of the entrance slit at the position of the exit slit. The wavelength is scanned by rotation of the grating. The exit slit is also the light entrance slit of the ion source. The light beam produces ions while passing through the ionization chamber, then leaves the ionization chamber through another slot and falls upon a sodium salicylate coated window. The fluorescence produced thereupon is sensed by a photomultiplier. The ions in the ionization chamber are accelerated onto an aperture and after leaving the ionization chamber are further accelerated and focused into the entrance slit of the magnetic analyzer. Depending on ion energy and magnetic field strength, one specific mass will be focused at the spectrometer exit slit and enter the ion multiplier. There the ion current is converted into an electron current, considerably amplified, and sensed by an electrometer.

A more detailed description of the several units employed follows.

The Mass Analyzer

In view of the small numbers of ions produced in a photo ion source compared with an electron impact ion source, a mass spectrometer utilizing this type of ionization requires a very high transmission. The ideal case would be reached, if all the ions of one mass which leave the extraction opening of the ion source are also passed through the entire analyzer. In addition to these transmission requirements and to obtain as much information as possible, it was necessary to have a resolution as high as feasible. The most suitable solution to this problem is a 180-degree magnetic analyzer which utilizes an inhomogeneous magnetic field between a wedge-shaped air gap. The theory of this instrument is well described in the literature [11,12], but surprisingly, it has only been used in β-spectrometry [12].

In our design, entrance and exit slits are six inches apart; thus, the mass spectrometer may be compared to a conventional 180-degree analyzer with a three-inch radius. However, because of the wedge-shaped air gap and the accordingly inhomogeneous magnetic field, the ions move on a cycloidal rather than a circular orbit. The entrance and exit slits are outside the magnetic field at a location very close to the line where the extension of both planes of the pole faces intersect. The distance from each slit to the magnetic

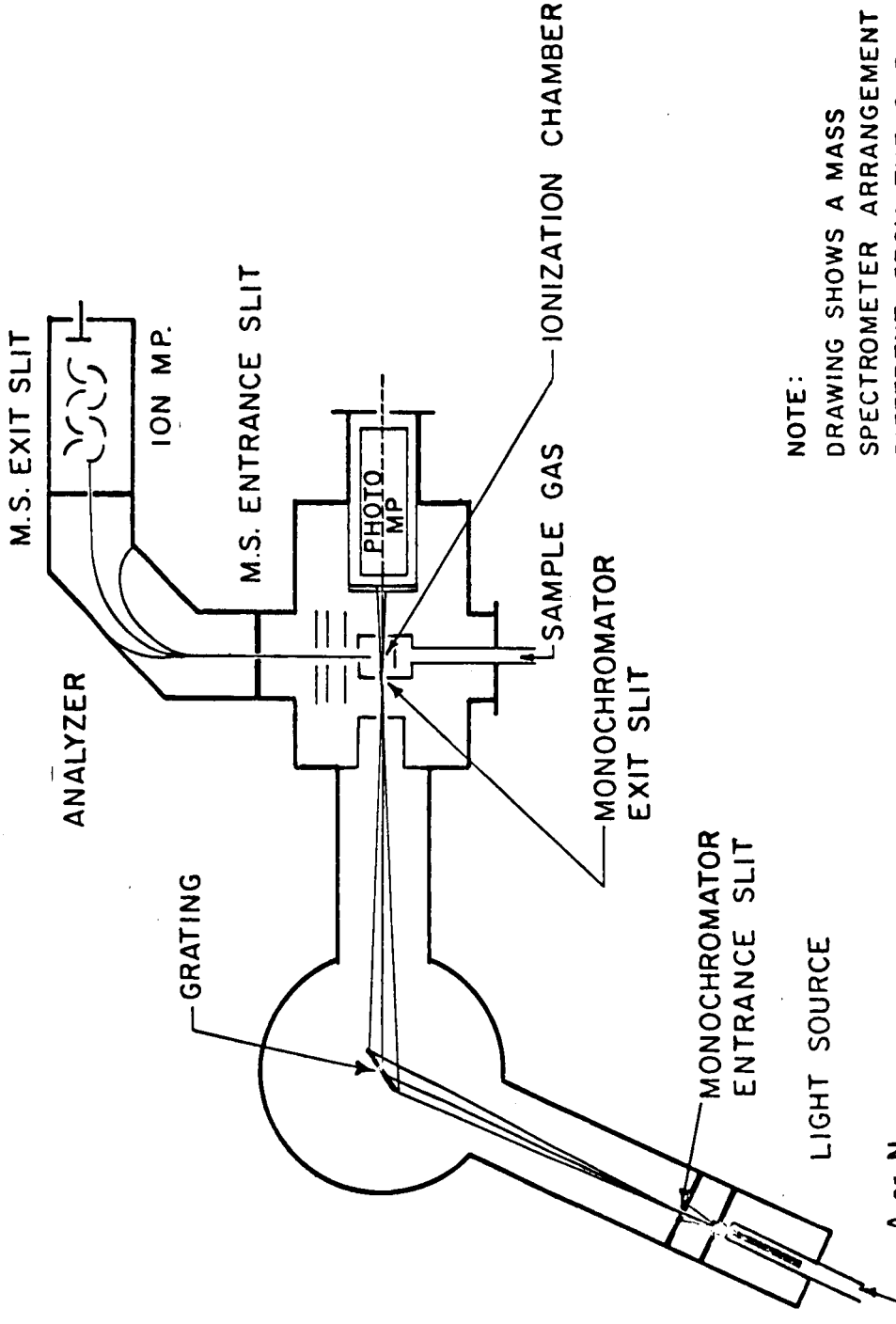

Figure 1. Principle arrangement of a photoionization mass spectrometer.

field boundary is given by the theory as 2.24 in. for the chosen distance of 6 inches between the apertures and with consideration of the fringe field effects. The fringe field conditions are defined by Herzog [13] shunts. The angle of inclination between the two pole faces is 12 degrees. The actual aperture available for the ion beam is defined by circular openings at the field boundary, and has been made somewhat smaller to prevent ions from striking the pole pieces. The effective collection angle corresponds to a cone with an opening angle of 10 degrees. The theory indicates that under the selected conditions fully stigmatic focusing occurs with the image aberrations in the center plane vanishing up to the fourth order [12]. In addition to this and due to the inhomogeneous field, the spectrometer has about 60 percent higher dispersion and accordingly higher resolution than a conventional 180-degree instrument of equivalent dimensions. The theoretical mass resolution of this device is calculated for 1 mm entrance and exit slits as $M/\Delta M = 65$ with a corresponding half width resolution of 130. The resolution of a comparable conventional mass spectrometer is about 40 - or 80 at half width. The allowable aperture is at best one degree and has no stigmatic focusing. This clearly indicates the superiority of the present design.

Mechanically, the analyzer consists of a box 2.5 x 3.5 x 7.5 inches, welded together from stainless steel plates and integrated with the wedge-shaped pole pieces made from special Armco mild steel. This box is fitted into the gap of an electromagnet with symmetrical coil arrangement. The magnet coils are water-cooled and dimensioned for a maximum current of 10 amperes at 36 volts when switched in series. This provides a maximum of 9000 ampere turns and the corresponding magnetic induction is about 4000 gauss in the center portion of the analyzer gap. For an ion energy of 1000 eV the mass range is from 1 to 50. For 200 eV ions the mass range goes from 1 to 250, since at a fixed magnetic field the mass focused onto the exit slit is inversely proportional to the acceleration voltage.

The rather heavy (220 pounds) magnet-spectrometer assembly is mounted on a sturdy double carriage which is precisely guided by ball bushings running on 3/4-inch diameter steel rods. Connection to the ion source housing is via stainless steel bellows. Thus, accurate adjustment of the spectrometer with respect to the ion source and entrance slit is facilitated.

The exit slit assembly comprises an adjustable exit slit and a suppressor arrangement, and is welded onto the mass spectrometer. A micrometer adjustment for the exit slit allows the selection of slits of different dimensions and also permits change of the location with respect to the center plane of the analyzer. (It should be mentioned here that the term "slit" is used with regard to conventional mass spectrometers to avoid confusion. However, since our instrument employs stigmatic focusing, the "slits" are holes of circular or square shape.) The suppressor arrangement located behind the exit slit also departs from the usual structure. To some extent it resembles a tubular einzellens with a mesh grid at one end of the center electrode. This specially designed arrangement has the advantage of giving a sharply defined limitation of the transmitted ion energy without the usually found change of the effective beam aperture and the corresponding effect on the focusing of the beam onto

the first dynode of the multiplier. It also allows the determination of the energy of the ions far more accurately and without ambiguity, since the voltage applied to the center lens is identical with the real retarding potential.

A collector for monitoring the total ion current is mounted on a straight line behind the entrance slit. Ions of all masses are simultaneously collected there if the magnetic field is switched off.

Ion Source

The arrangement of the ion source is shown in Figures 2 and 3. The light coming from the monochromator at first passes a wider slit which acts as a baffle. This latter slit also serves to maintain a pressure differential between the ion source housing and the monochromator. Integrated with this slit is an appropriately biased electrode system which deflects any photoelectrons coming from the grating or from elsewhere in the monochromator, and it also collects photoelectrons produced at the actual ion source entrance slit. Thus, no photoelectrons can enter the ionization chamber. The light enters the ionization chamber through an adjustable entrance slit also located in the focal plane of the monochromator. The light beam leaves the ion source through a slot sufficiently wide to prevent the formation of photoelectrons from the photon that may strike the walls. The slot is used here rather than a slit because it reduces the gas flow out of the ion source. After the light beam has passed through the ion source, it falls upon a sodium salicylate-coated glass plate viewed by a photomultiplier. Dibeler and Reese [8] stated that the quantum yield of the coating is affected by exposure to hydrocarbon vapors. However, no such effect has been observed in the present work or in other work performed at GCA under comparable conditions. Although the photoelectric detector used by Dibeler and Reese [8] allows the determination of absolute photon fluxes, preference has been given to the sodium salicylate converter because its quantum yield is approximately constant over wide wavelength regions [14] and the use of a photomultiplier provides a simple and fast electronic readout. Intensity comparisons are thereby facilitated.

Owing to the stigmatic focusing properties of the mass analyzer, the ion source geometry has been made cylindrical, coaxial with the center of the ion beam. This also permits a simple, neat, and sturdy construction. Special care was given to the design of the ionization chamber. The ion repeller and the ion extraction electrode are spherically shaped. This results in a radial field which accelerates the ions mainly toward the extraction hold and accordingly increases the available ion current. The repeller can be adjusted externally by a micrometer screw and can be moved as close as possible to the ionization region. Thus the potential drop across the ionization chamber can be kept small and no electron can gain energy high enough for ionization. Similarly, the extraction electrode is brought close to the ionizing light beam so that the residence time of ions can be minimized in the high pressure region of the ion chamber. This arrangement suppresses ion-molecule collisions which can result in unwanted charge exchanges and ion-molecule reactions [15]. Repeller and extraction electrodes are electrically insulated from the other

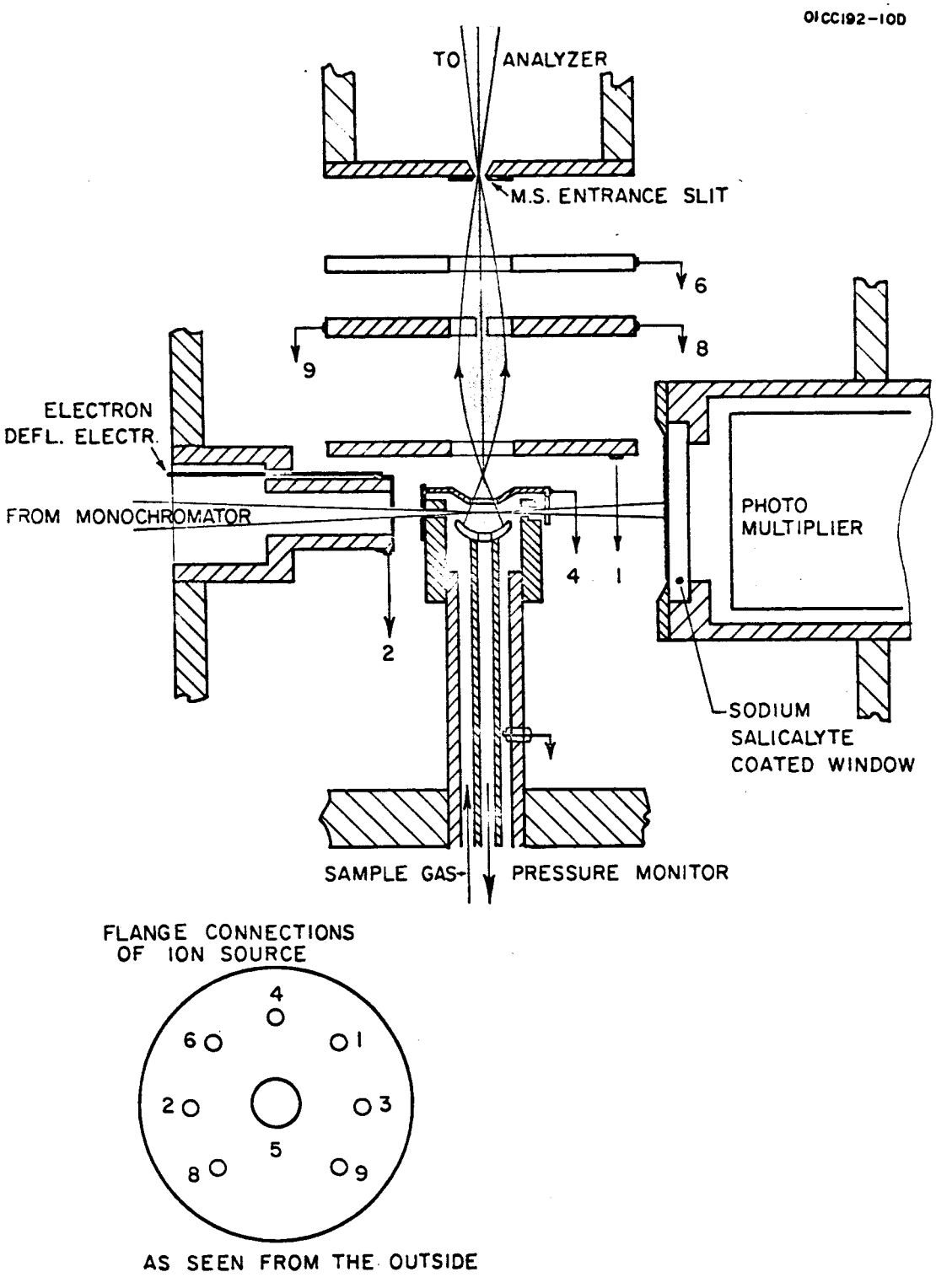

Figure 2. Principle and schematic of photoionization ion source.

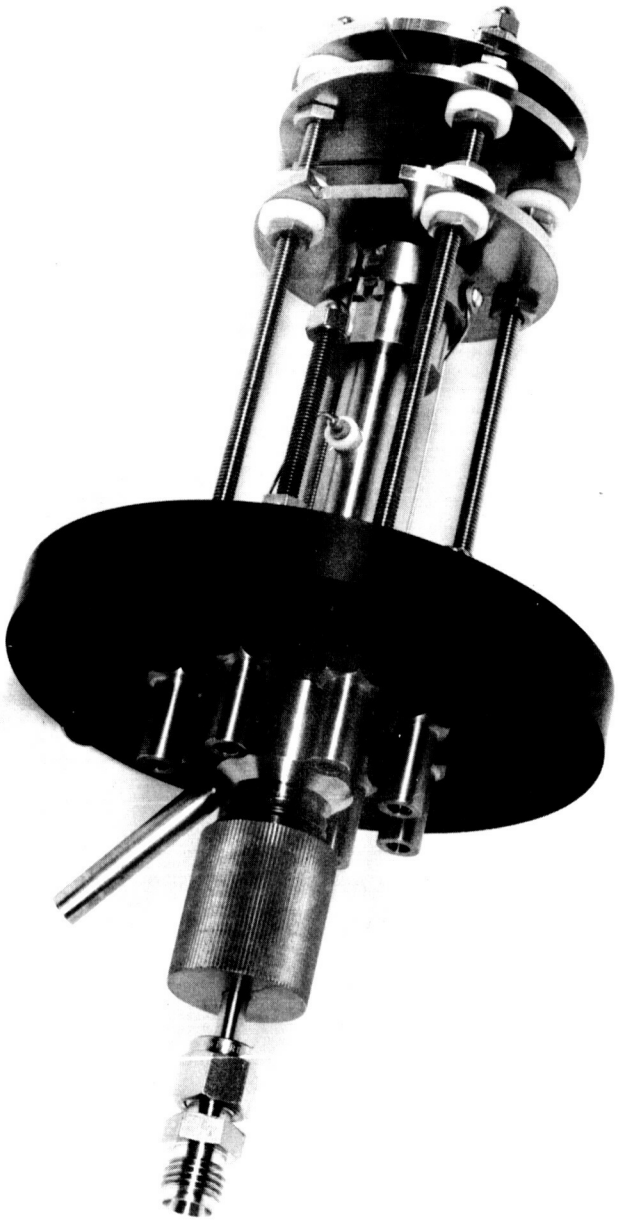

Figure 3. Ion source.

walls of the ionization chamber, and the relevant potentials can be adjusted to guarantee highest ion emission efficiency. (If a wide extraction opening of 1/4 in. diameter - such as in our experiments - is used, the field penetration from the acceleration field alone gives the most efficient ion extraction. For the study of ion-molecule reactions, however, higher pressures in the ionization chamber and a longer traveling distance for the primarily formed ions to the extraction opening have to be used. This necessitates a smaller extraction hole to maintain the pressure in the ion source housing below 1μ and also requires a longer distance from the intersecing ionizing light beam to the extraction opening. In this case, the field penetration from the acceleration field is negligible and an internal field has to be applied which for these studies should be well defined and known. The independently variable potential of the repeller and the draw electrode provide the highest versatility of the instrument.) The ions leaving the reaction chamber are accelerated and focused onto the analyzer entrance by an immersion lens system consisting of three plates with 1/2 in. openings. The potential of the first plate affects the focal length. The two following plates are divided into halves and permit adjustment of the ion beam in vertical and horizontal direction. These two plates are kept on a negative potential with respect to ground. Therefore, secondary electrons conceivably formed by interaction of the ion beam with the analyzer entrance slit are prevented from being accelerated back into the ion source. The holes in the lens plates are sufficiently wide to prevent ions from striking there and releasing electrons.

The pressure in the ion chamber is accurately sensed by a separate pipe connection which ends in the center of the repeller disc. The sample gas is fed into the reaction chamber through a pipe concentric to the pipe mentioned before.

The whole structure is mounted on a completely opaque nylon flange and all feedthrough connections are sealed with viton O-rings. All parts in contact with the gas or the ion beam are stainless steel. Assembly, cleaning, and adjustment are very simple.

The gas is fed to the ion source via teflon tubing. This provides the necessary insulation between the potential of the ion source and the grounded needle valves. Two needle valves regulate the gas flow and permit mixing of two gas components. Seals in this part are made with Swagelok couplings.

Ion Detector

A commercial Nuclide Corporation multiplier, type EM-2, with 16 stages is used for the detections of the ions leaving through the exit slit of the magnetic analyzer. It utilizes a pie-type arrangement of activated BeCu dynodes. The nominal gain is specified between 10^5 and 10^6, and the noise level corresponding to an input of less than 10^{-19} amperes.

Figure 4 gives the multiplier gain as a function of the multiplier voltage. It should be noted that the mass and the energy of the ions are quite

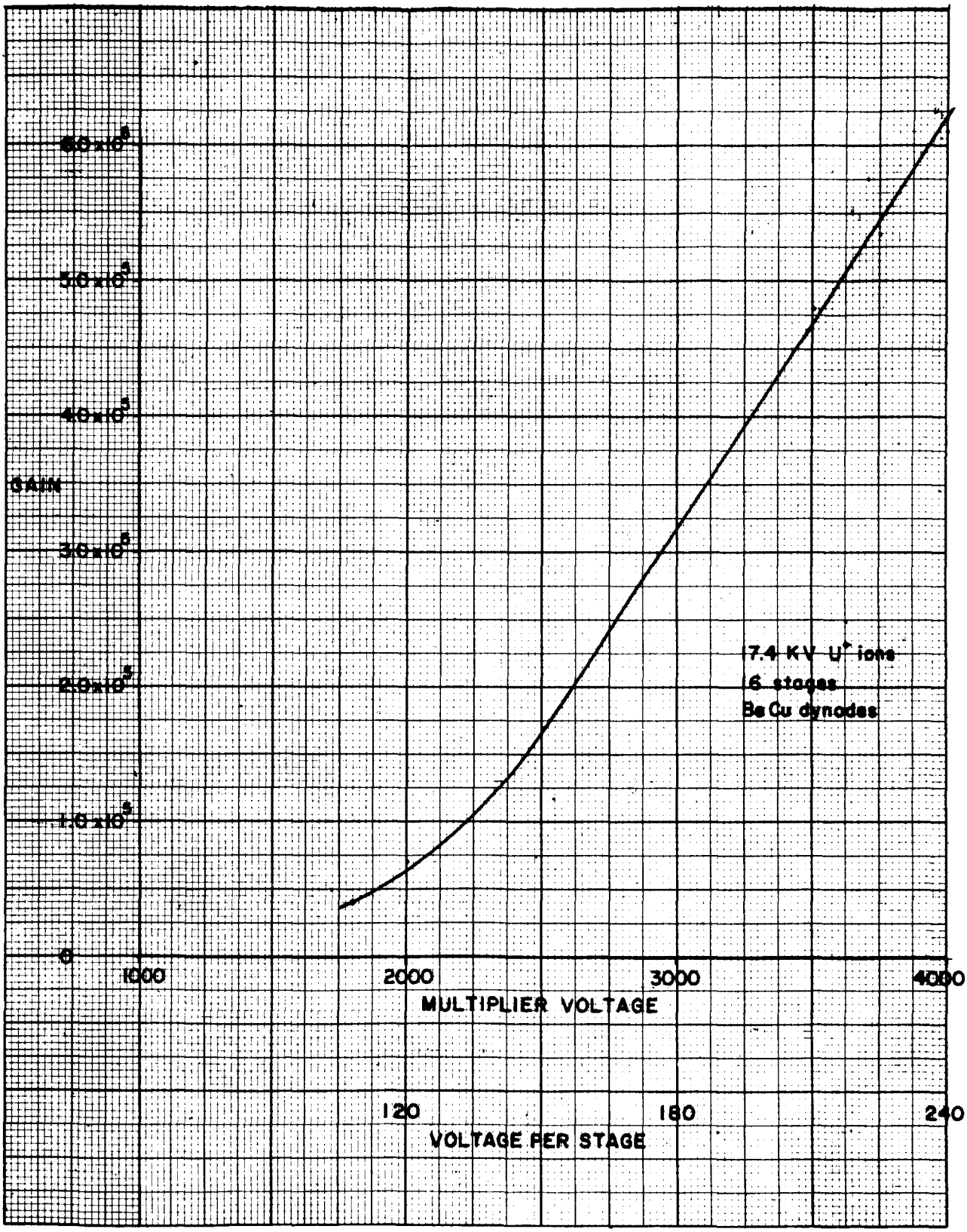

Figure 4. Overall multiplier gain vs multiplier voltage.

different. The ion energy is given by the acceleration voltage in the ion source plus the acceleration between exit slit and first multiplier dynode since the first dynode is on a high negative potential, about identical with the multiplier voltage. The mass range is between 1 and 50 and the ion energy is 3.5 keV. However, this will affect the gain by less than half an order of magnitude. External and well insulated connection is provided for the high voltage lead, collector lead, and for the ground lead. This allows measurement of the ion current falling onto the first dynode with an electrometer connected to the high voltage input, and the ground lead left floating.

The multiplier is encased within a magnetic shield and mounted in a stainless steel housing which is flanged to the exit slit assembly of the mass spectrometer.

All electrical connections into the vacuum are made with Alite feedthroughs combined with BNC connectors and are well shielded. The multiplier voltage should not exceed 3000 volts. A lower voltage provides sufficient amplification and was found to give a better signal-to-noise ratio.

Light Source

The light source, built under the contract and used for the measurements, is a repetitively pulsed spark discharge using a ceramic capillary. This source is similar to that described by Weissler, et al. [16]. It works well with most permanent gases and emits a rich spectrum of widely spaced lines mainly in the region 400 to 1000Å with maximum intensities comparable to those of the rare gas resonance lines. The working pressure is typically around 50μ Hg, which is 10 times less than the working pressure of a dc discharge. This means lower gas consumption and less gas flow into the monochromator. Figure 5 shows the light source and a cutaway of the instrument is shown in Figure 6. The outer parts are made out of copper to achieve high electric and heat conductivity. Anode and cathode and all points where sealing viton O-rings are located are very effectively water cooled. The hollow anode and the cathode cap are Elkonite, an alloy which resists sputtering particularly well. The capillary is Boron Nitride, a machineable ceramic. The discharge can be viewed through an observation window at the end.

The spark source requires only a few minutes of operation to stabilize and can work continuously over many hours. Intensity fluctuations usually stay within one percent, provided the other parameters, such as pressure and voltage stay constant. Cleaning and assembly is very simple; the construction is self-adjusting.

Monochromator

The monochromator system was supplied by GCA for the tests and is not a deliverable item under the contract. It is a McPherson 1/2-inch Seya instrument, fitted with a 1200 lines/mm tripartite replica grating blazed for 750Å.

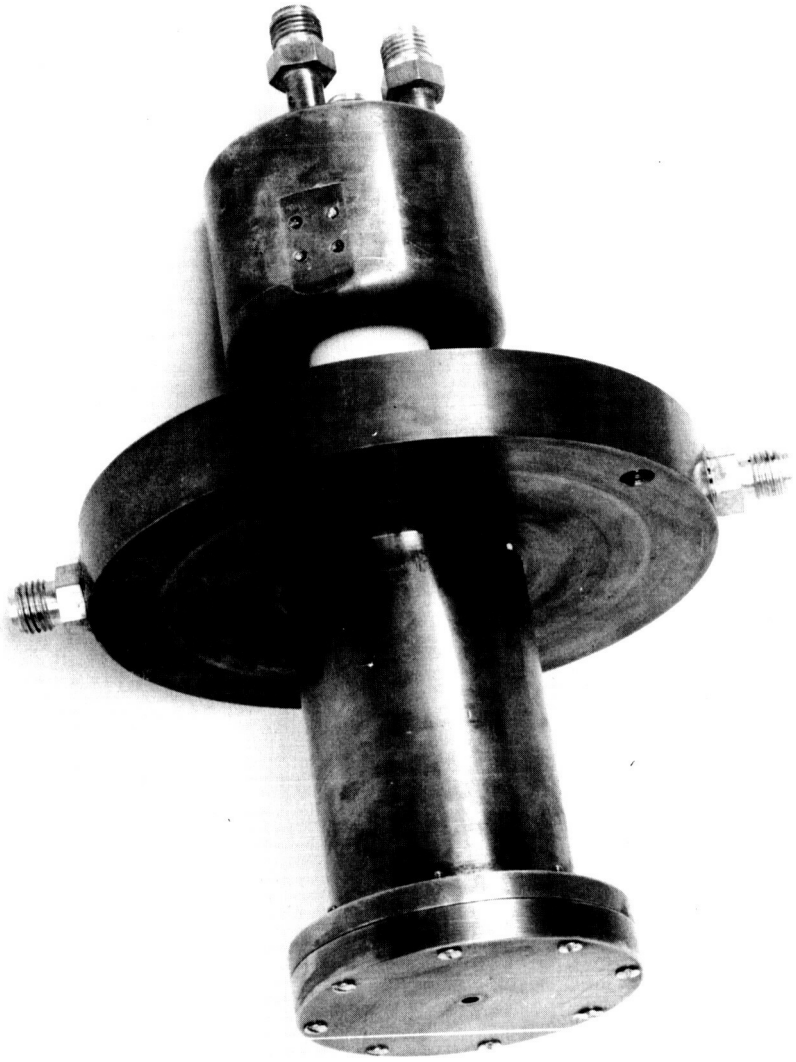

Figure 5. Light source.

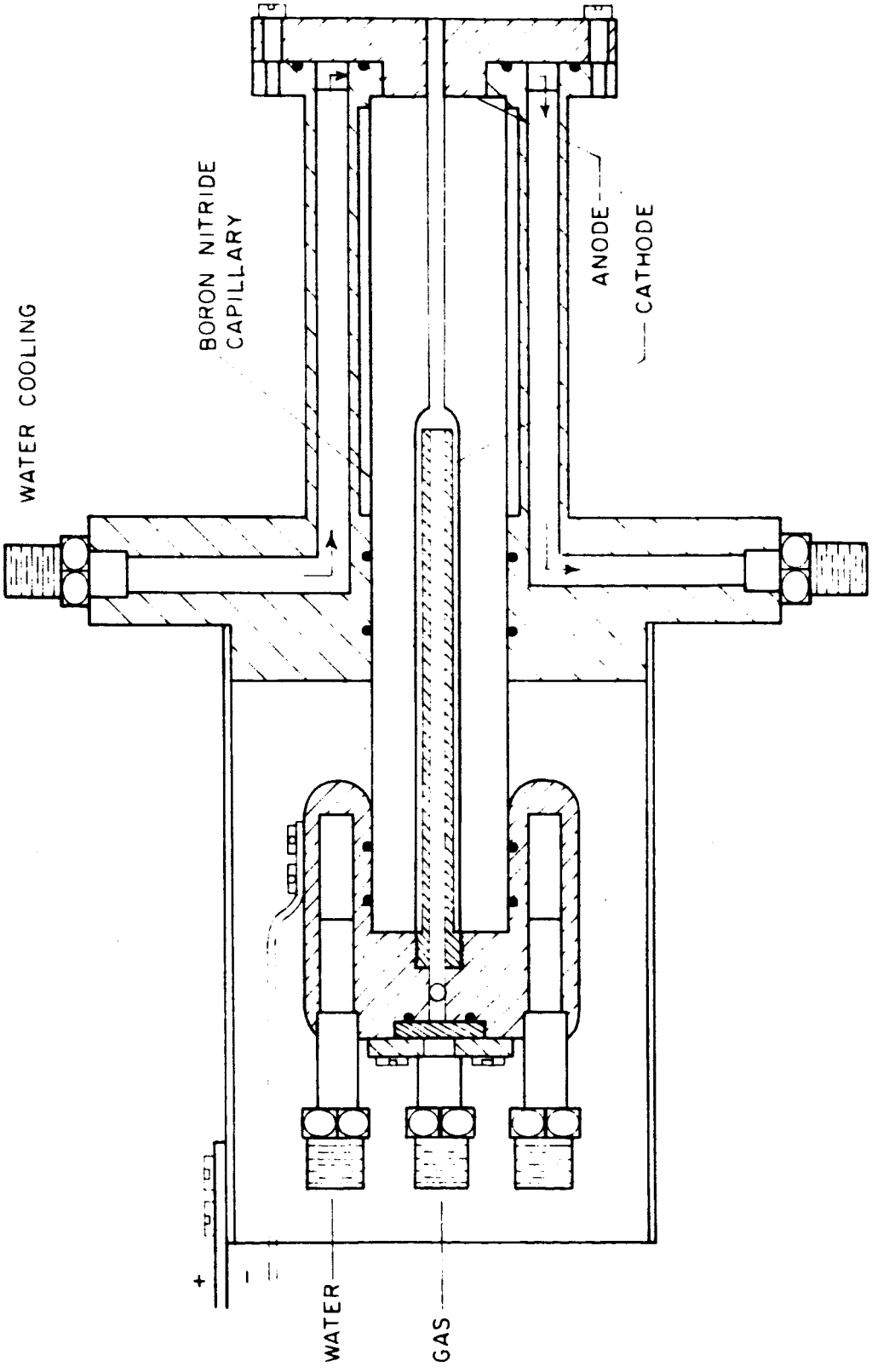

Figure 6. UV spark source.

The head bearing of the exit slit assembly was removed from the exit arm of the monochromator and replaced by the tubular adapter section which is part of the ion source housing. The optical entrance slit of the ion source serves as the new monochromator exit slit. With the slit jaws set to a width of 250 microns, the observed wavelength resolution was approximately 5Å. At 750Å, this corresponds to an energy resolution of 0.1 eV. The monochromator is mounted on a table which matches the mass spectrometer table and as such is a completely self-contained system.

Vacuum System

The key to a successful operation of the integrated apparatus is the application of differential pumping. Light source pressures are between 50 and 100 microns, while the monochromator chamber should be kept at pressures below 10^{-4} torr to avoid losses from optical absorption. Similarly, it is desirable to operate the ion source at pressures up to 20 microns, whereas in the mass analyzer chamber, pressures much above 10^{-5} torr cannot be tolerated because of ion beam scattering. These requirements are met by the following pumping stages: The monochromator has its own baffled diffusion pump which develops a pump speed of 350 liter/sec. Between light source and monochromator is a buffer chamber which is also pumped differentially with a 375 liter/min mechanical pump. The ion source housing is evacuated by a baffled 4-inch nominal oil diffusion pump at 350 liter/sec. This maintains the pressure in the ion source housing below the pressure in the ionization chamber by approximately a factor of 100. The mass analyzer, finally, is evacuated by a 2-inch diffusion pump also fitted with a baffle and is easily kept two orders of magnitude below the pressure of the ion source housing. All diffusion pumps can be backed up by a single 375 liter/min mechanical pump. All baffles are of the "multi-coolant" type. Water cooling has proven to be sufficient, but freon or liquid nitrogen may be used.

As an example of the efficiency of the described arrangement, pressures observed with an ion source pressure of 20μ are: light source 50 microns; monochromator 2×10^{-5} torr; ion source housing 4×10^{-4} torr, analyzer chamber 3×10^{-6} torr.

Normally, it is only necessary to sense the pressure at the light source, at the ionization chamber, at the mass spectrometer, and in the foreline. For this purpose, a GCA Type 902 pressure control system is supplied for the instrument.

Mechanical Construction

The total arrangement comprises three heavy main components with weights between 80 and 250 pounds; namely: monochromator, ion source housing, and mass spectrometer. Because these parts have to be accurately adjusted and must stay in alignment with respect to each other, specific care has been given to the mechanical design.

The monochromator is a self-contained system mounted in a sturdy steel table, which aligns with and is firmly bolted to the spectrometer table.

The ion source housing together with the photomultiplier subassembly, the baffle, and the diffusion pumps is supported by a spring-loaded frame. By adjustment of the spring tension, the whole unit can be kept floating at the right height and position. This permits precise adjustment without undue stress on the interconnecting parts.

After the ion source has been adjusted, the mass spectrometer has to be aligned with respect to the ion source housing, which also contains the analyzer entrance slit. Accurate adjustment is facilitated by the precisely guided, sturdy carriage onto which the mass spectrometer is mounted. Adjustment is provided in all three dimensions. A very flexible welded stainless steel bellow interconnects the spectrometer with the ion source housing. This allows freedom of movement with respect to each other and avoids mechanical stress. A special clamped flange connection affords rapid and easy detachment of the mass spectrometer from the ion source housing. In addition, the movable spectrometer carriage can be shifted sufficiently to make all parts accessible for servicing. Figure 7 shows the arrangement.

Electronics

Commercially available electronics are mainly used with the instrument. The only exceptions are the ion source voltage supply and the spark gap. The simplified schematic given in Figure 8 essentially shows a voltage divider string tapped at several points through potentiometer arrangements which provide the appropriate range of voltage. A zener diode is used to fix the repeller and draw electrode potential independently from the amount of total voltage applied. While all other voltages should be proportional to the total voltage, the field condition in the ionization chamber should be an independent parameter. The lens electrodes for the vertical and horizontal adjustment of the ion beam are at a negative potential with respect to ground. This is achieved by grounding the voltage divider at an in-between point which requires a high voltage power supply with floating output. A regulated high voltage power supply, Fluke 412B1 AF, 0 to 2100V, 0 to 30 mA is used for this purpose.

Two additional Fluke high voltage power supplies of type 412B, 0 to 2100V, 0 to 30 mA and type 408B, 0 to 6000V, 0 to 20 mA are used for the photomultiplier and ion multiplier, respectively.

The magnetic current power supply is a Kepco KS 36-10M with a maximum current of 10 A and a maximum voltage of 36 volts. The magnetic current is scanned by a motorized programmer (Kepco MP-1-3000-5K) which provides the mass scan. Eight scanning speeds are available from 3000 sec to 1 sec for a current change of 0 to 10 A. The power supply is regulated to 0.01 percent and provides adjustable voltage or current regulation in a unique cross-over arrangement.

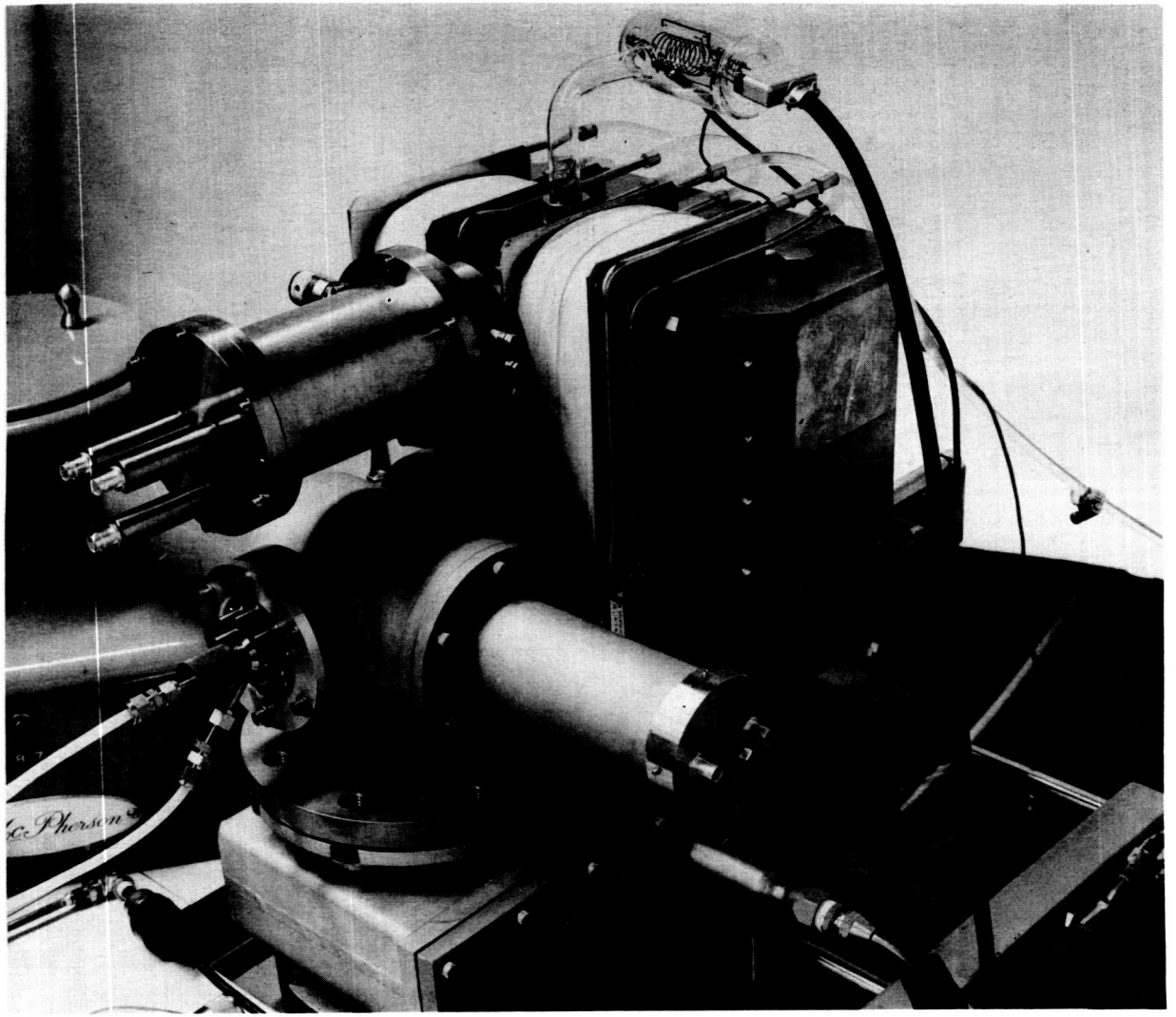

Figure 7. Analyzer closeup.

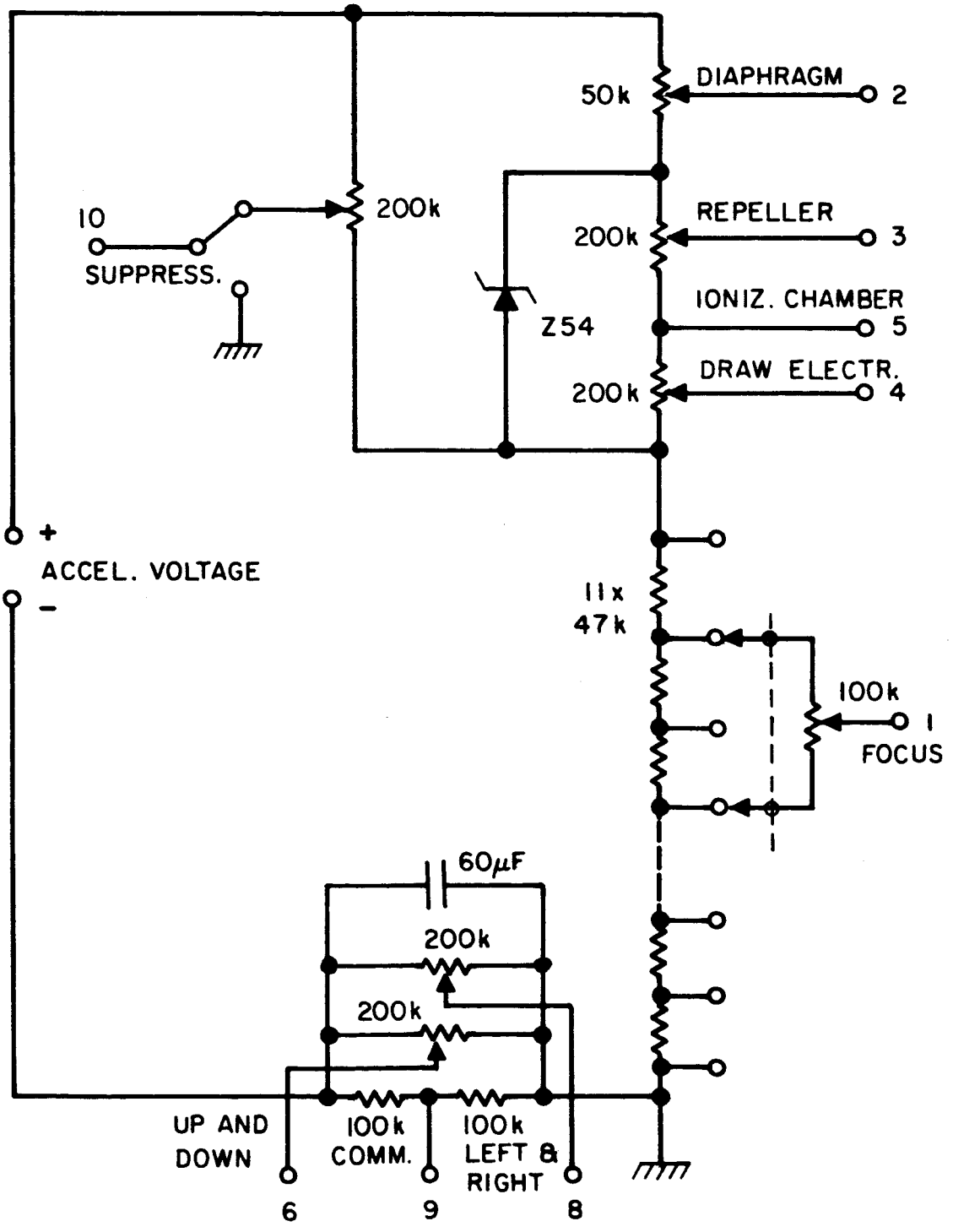

Figure 8. Ion source voltage supply.

The power for the uv spark source is supplied by a NJE H5 200 high voltage power supply. It has an output of 0 to 5000 volts and 200 mA and is regulated to 1 percent. Trip controls for over voltage and over current are provided. The voltage is pulsed by a rotary spark gap designed by GCA. The schematic is shown in Figure 9. A 0.25μF high voltage capacitor is discharged at a rate of 120 times a second by a rotary spark gap driven by a synchronous motor. The spark gap is illuminated by a mercury quartz lamp which considerably increases the stability of the spark in the gap. The power is fed to the light source by a special coaxial cable. The spark gap circuitry is contained in a carefully shielded box that is cooled by two fans.

The output from the multipliers or from the total ion current collector is sensed by a high speed pico ammeter (Keithly Model 417). The electrometer features a remote preamplifier which can be brought close to the sensing point.

Also used for the experiments were some additional GCA owned equipment such as a speedomax recorder and an additional pico ammeter. The latter was used to monitor the output from the photomultiplier. For some experiments, an additional recorder was used. This enabled us to record the signal from the photomultiplier simultaneously with the signal from the ion multiplier while the wavelength was scanned with the monochromator.

Figure 10 shows the complete system.

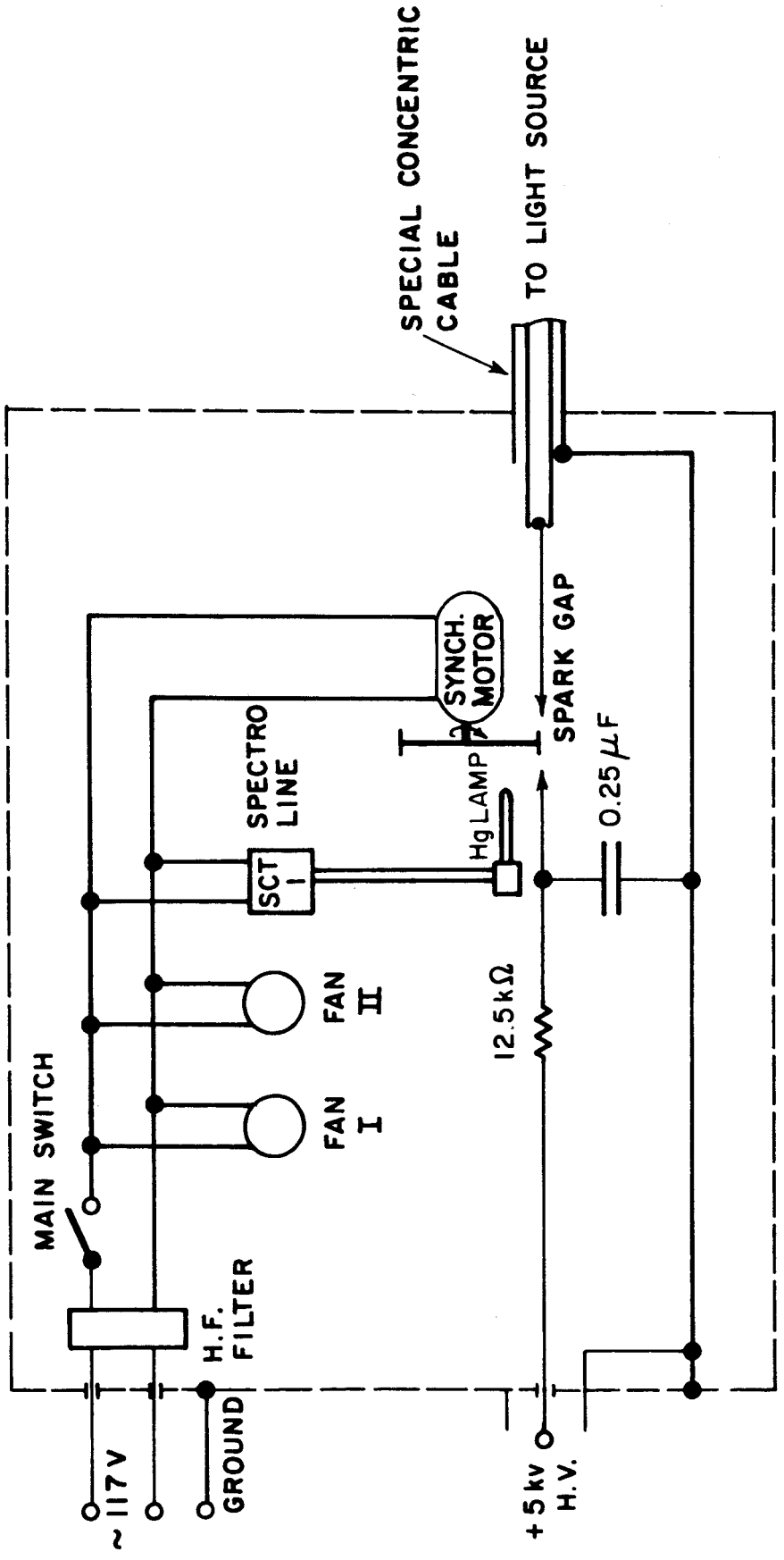

Figure 9. Rotary spark gap.

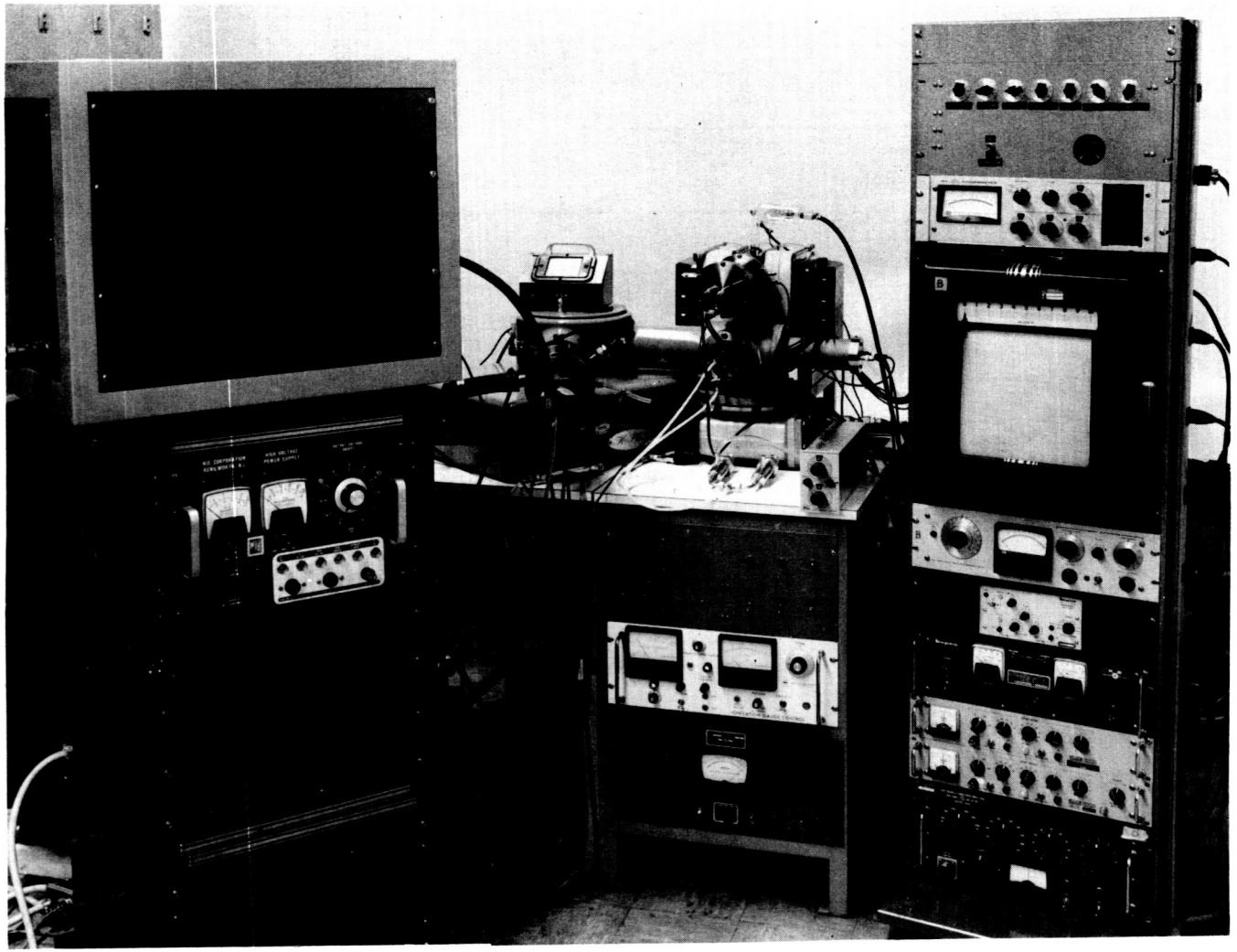

Figure 10. Overall view of photoionization mass spectrometer.

EXPERIMENTAL

Handling the Instrument

The instrument may be used as soon as the pressure in the mass analyzer has reached 1×10^{-5} Torr, but it is advisable to wait until the pressure is down below 2×10^{-6} Torr. The lowest pressure reached with this system, using water cooled baffles only, is 4×10^{-7} Torr. When the instrument was not previously vented, this pressure was attained three hours after the start of the diffusion pumps. When the system is not used and the diffusion pumps are switched off, the foreline valves should be closed. The system should never idle on only the forepumps since this will cause forepump oil to contaminate the system and limit the base pressure.

After the vacuum conditions are satisfactory, the light source is started. First, the cooling water is turned on and with a needle valve control, gas is fed into the light source until an equilibrium pressure of about 50μ Hg is reached, measured at the buffer chamber.

Next, the spark gap unit is switched on and the high voltage power supply slowly turned up to about 5 kV. The light source will draw between 60 and 80 mA. The discharge can be viewed through the observation window. After a few minutes, the light source should come to a good stable operation. If larger fluctuations still occur, either the gas pressure is too low or the rotary spark gap needs readjustment. Rotating the electrode pins in their holders will readjust the spark gap; however, if too much electrode material is burned off, the pins have to be replaced.

Next, a voltage of -750 V is applied to the photomultiplier and the multiplier collector is connected to the electrometer. Scanning of the monochromator should give a spectrum of the light source with peak currents in the 10^{-7} A range. A strong spectral line with an adequate wavelength to ionize the sample gas is selected. After this, the acceleration voltage is applied (+1000 volts for a mass range from 0...50). With the magnet current still off, the total ion current can be measured when the electrometer is connected to the total ion current collector. Depending on the pressure of the sample gas in the ion source (up to 20μ), the type of gas, and the special line selected, total ion currents are from below 10^{-14} A up to 5×10^{-13} A. Usually, it is not necessary to first check the total ion current, since the additional gain of the ion multiplier makes it easy to pick up the main peaks and to perform all the optimizing adjustments. An ion multiplier voltage between -2000 and -3000 volts is completely sufficient and will yield peak currents up to 1×10^{-8}A at the collector. Higher multiplier voltages will increase the output, but a strong increase of background spikes actually decreases the signal-to-noise ratio.

The experiments have shown that the alignment and adjustment of the system is not too critical. Since no extreme resolution is required from the monochromator, the exact "in focus" location of the monochromator exit - which is identical with the light entrance slit of the ion source - is not critical. Axial alignment of all light slits can easily be checked by visual observation of the central image from the grating, using a simple light bulb in front of the monochromator entrance slit. As long as no high mass resolution is required and the mass spectrometer is operated with wide slits (1 mm), the adjustment of the mass spectrometer is equally uncritical because of the high dispersion and the excellent focusing qualities of the instrument.

The only adjustments usually needed are the height position of the mass spectrometer exit slit and the potentials of the ion source. Both adjustments are more important with regard to the intensity even though for high resolution, the slit height adjustment will also affect resolution.

For the present ion source, it was found that best intensities are achieved with zero repeller and draw electrode potential with respect to the ionization chamber and with the highest potential drop applied between ion source and first acceleration electrode. The strong field penetration into the ionization chamber from the high acceleration field obviously results in the most favorable ion collection condition. The effects of small mechanical misalignments are compensated by the application of the electrostatic vertical and horizontal deflection to the ion beam.

Especially at higher pressures in the ion source, the mass peaks will develop tails toward the lower mass side, if the suppressor is switched off. These tails are due to ions which have lost energy by collision on a potential lower than the original ions. Since our suppressor arrangement guarantees a very sharp energy separation, all the secondary effect ions can be rejected. When the suppressor is switched on and its potential adjusted to a point where the peak intensity just starts to drop sharply, the tails will completely disappear.

Comparison of the uv-Spectrum of Nitrogen and Argon

During our investigations, the uv-spark source was run with argon and nitrogen. The light source works equally well with both gases, the differences lying in the spectral distribution of the intensity only. Figure 11 gives the uv-spectrum of N_2 between 430 and 930Å and Figure 12 the equivalent spectrum for argon. Comparison of the spectra shows that the argon produces a spectrum much richer in intense lines than nitrogen. The difference is particularly apparent at shorter wavelengths below 700Å, where argon still produces a big number of intense lines in

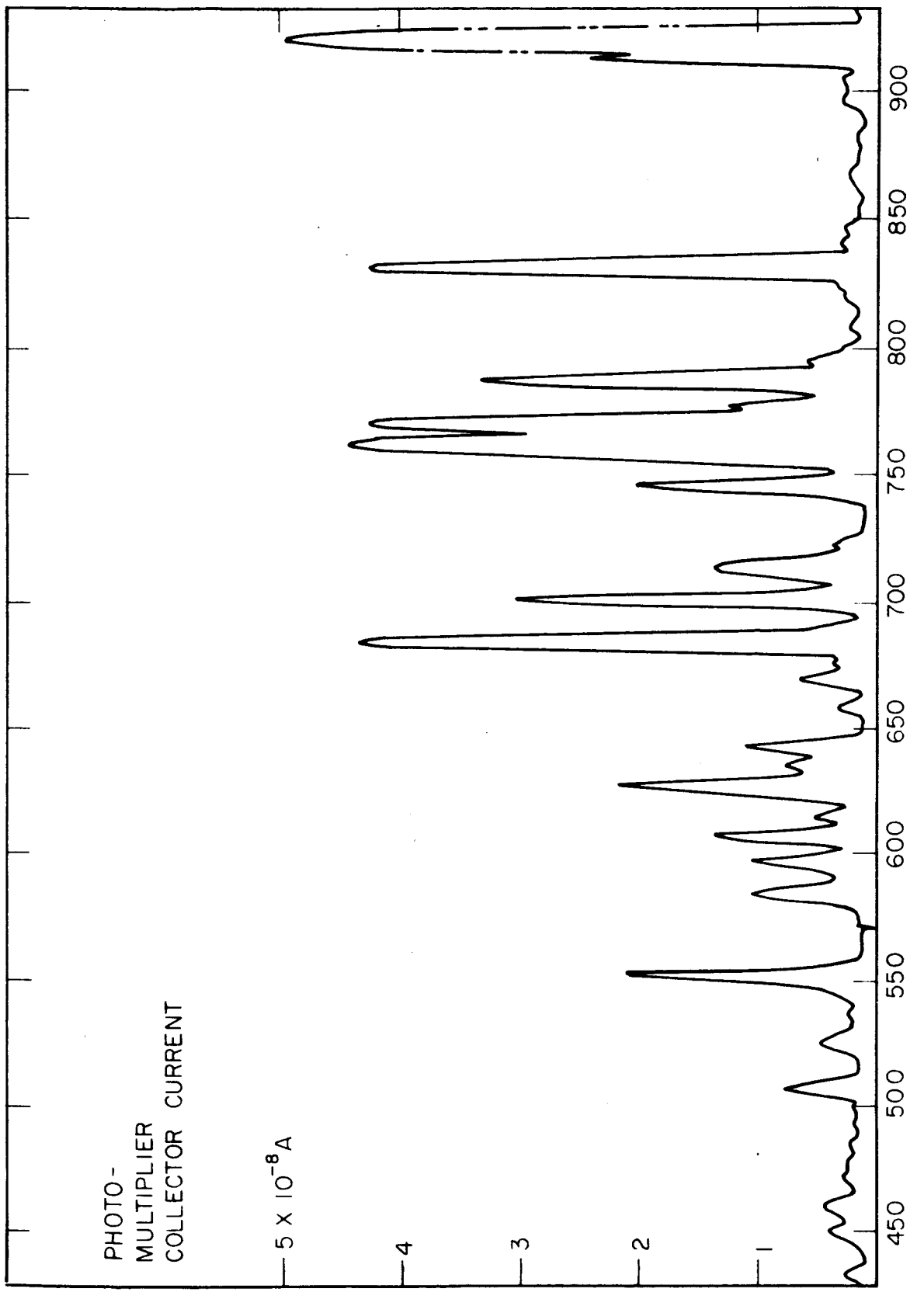

Figure 11. Nitrogen spark source spectrum – 30μ, 4.75 kV, 75 mA, photomultiplier 750 volts.

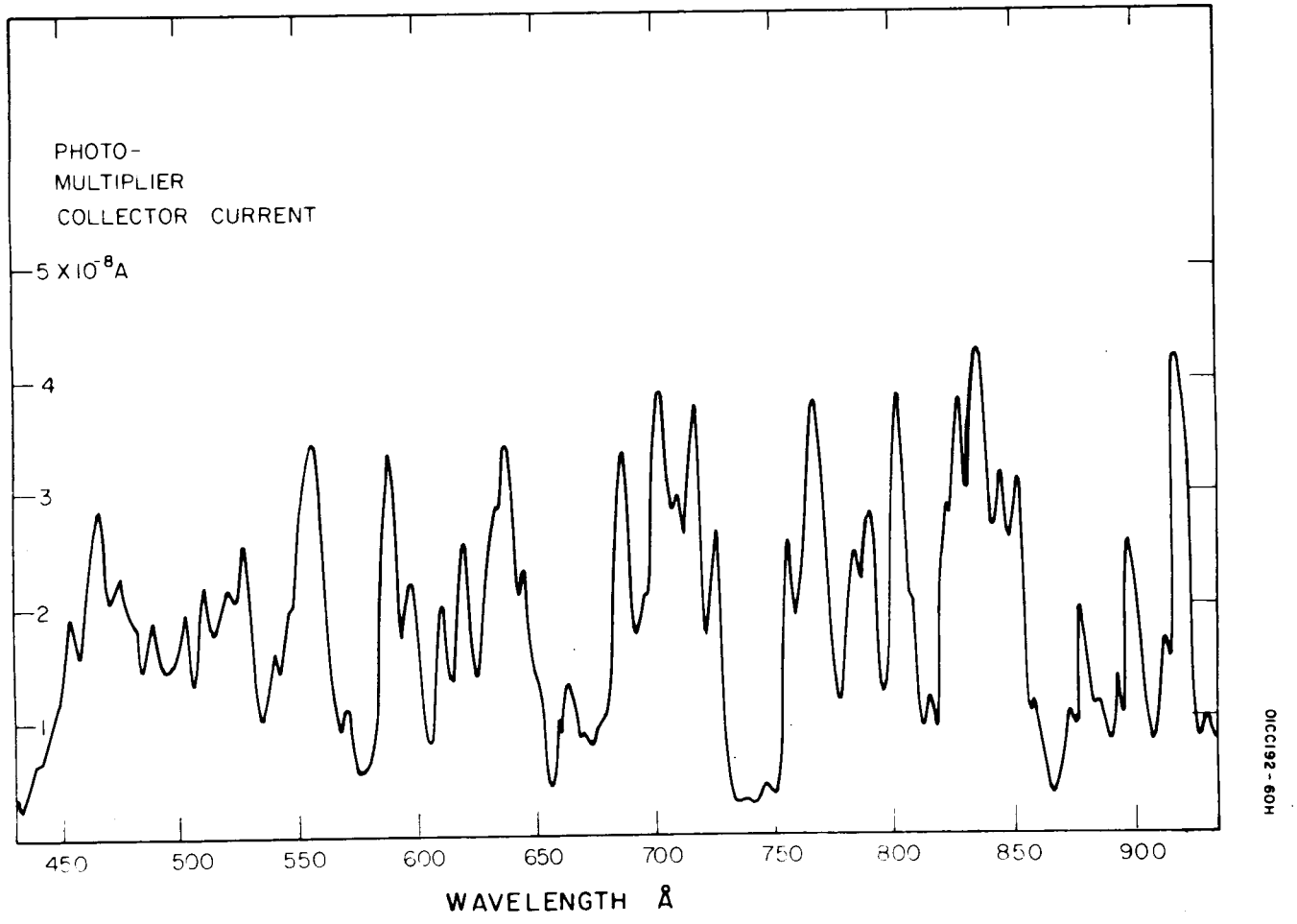

Figure 12. Argon spark source spectrum — 30μ, 4.76 kV, 75 mA, photomultiplier 750 volts.

contrast to N_2. Generally, one might conclude that argon gives the more favorable spectrum. However, as will be discussed later, with the present capabilities of our monochromator, the N_2 spectrum is more suitable if the separation of two gases at the same mass number is concerned.

Performance of the Mass Spectrometer

Figure 13 shows one of the first spectra obtained with the instrument. It is the spectrum of air ionized with the 788Å line of the argon spark spectrum corresponding to an energy of ca, 16 eV. This line yields a particularly high ionization rate of N_2, since near the threshold energy sharply defined resonance absorption occurs which results in very efficient ionization. The pressure in the ion source was 0.8μ and the pressure reading at the analyzer was 6×10^{-7}. The spectrum clearly delineates H_2O, $^{14}N_2$, $^{16}N^{15}N$, $^{16}O_2$, $^{16}O^{17}O$, $^{16}O^{18}O$, A, and CO_2. There is also an indication of atomic ^{16}O and ^{14}N. These actually should be omitted since the selected ionizing wavelength does not suffice to produce atomic O and N. This effect will be discussed later. The lines show small tails at the low mass side because the suppressor was not switched on. The tail on the high mass side is caused by the electrometer time constant only. For this first run, a Cary vibrating reed electrometer was used with an input resistance of $10^{11}\Omega$. The high noise level in the 300 mV range was due to high frequency pick-up from the spark source, although everything was well shielded. Subsequently, improved grounding with heavy copper brading considerably improved the spectra as can be seen from later figures.

Figure 14 gives a background spectrum obtained without any gas admittance to the ion source. The size of the N_2 peak indicates a background pressure in the ion source of about 3×10^{-5}, which suggested a small leak in the gas inlet system or the pressure monitoring line. (Actually, the Hastings gauge which was used to measure the ion source pressure was leaking slightly).

The resolving power, with proper adjustment of the suppressor voltage, is demonstrated on $^{14}N_2$ and $^{15}N^{14}N$ in Figure 15. The half-width resolution determined from there is about 120, which agrees well with the theoretical value for 1 mass entrance and exit slits. The shape of the valley between both peaks suggests at least a 0.01 percent valley, since the 28 peak is more that 100 times as intense. The clearly defined onset of the lines shows the fine performance of the mass spectrometer. From Figure 15, we can also derive a resolution of 65 for a 10 percent valley and of about 50 for a 1 percent valley definition. Figure 15 also shows an indication of a mass peak at 30 which is due to $^{15}N_2$ and corresponds to 16 ppm of $^{14}N_2$, demonstrating the sensitivity.

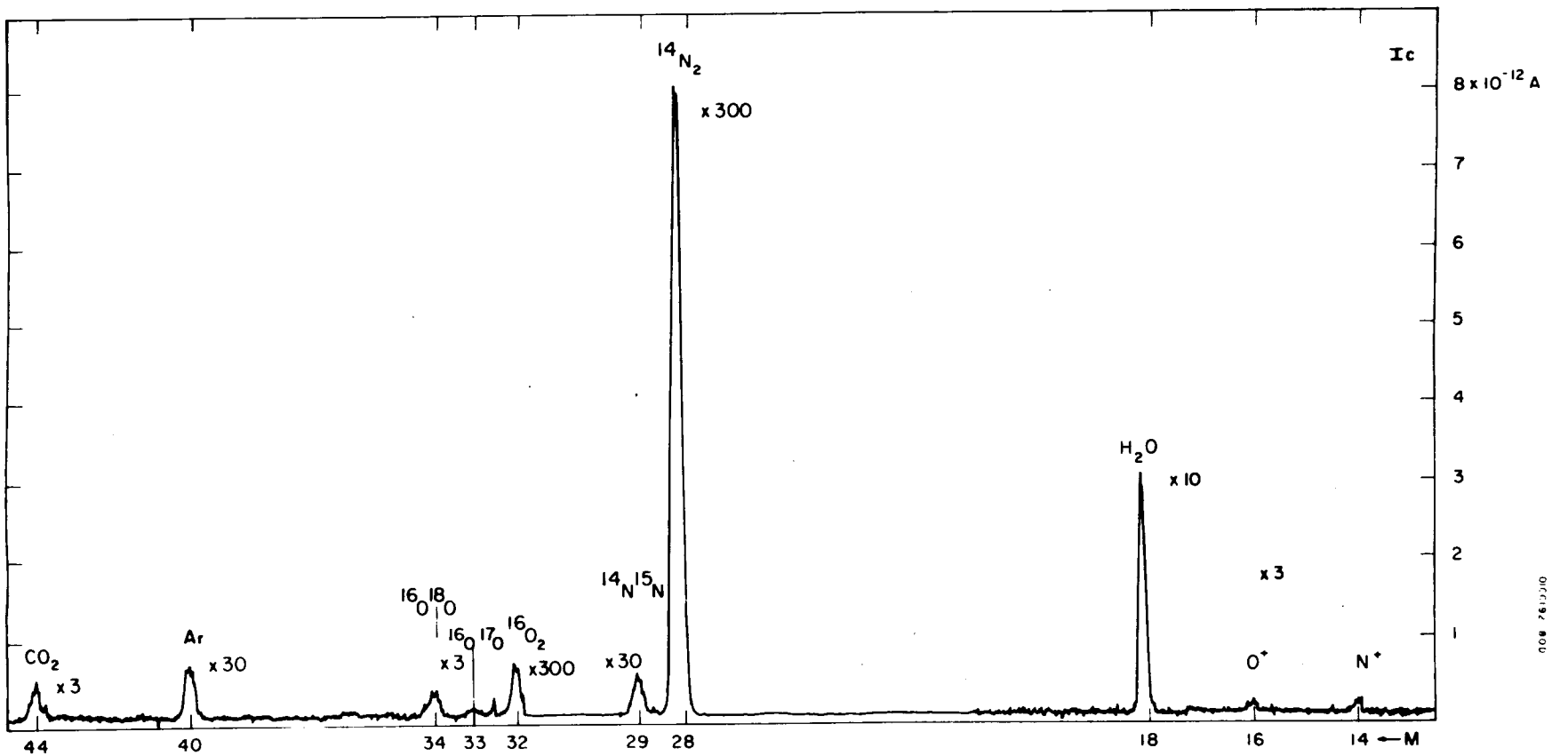

Figure 13. Air spectrum M = 14 to 44 — 1200 V acceleration, 788Å argon spark source, $P_s \approx 1\mu$ air, $P_A = 8 \times 10^{-7}$ Torr, ion multiplier: 2000 volts.

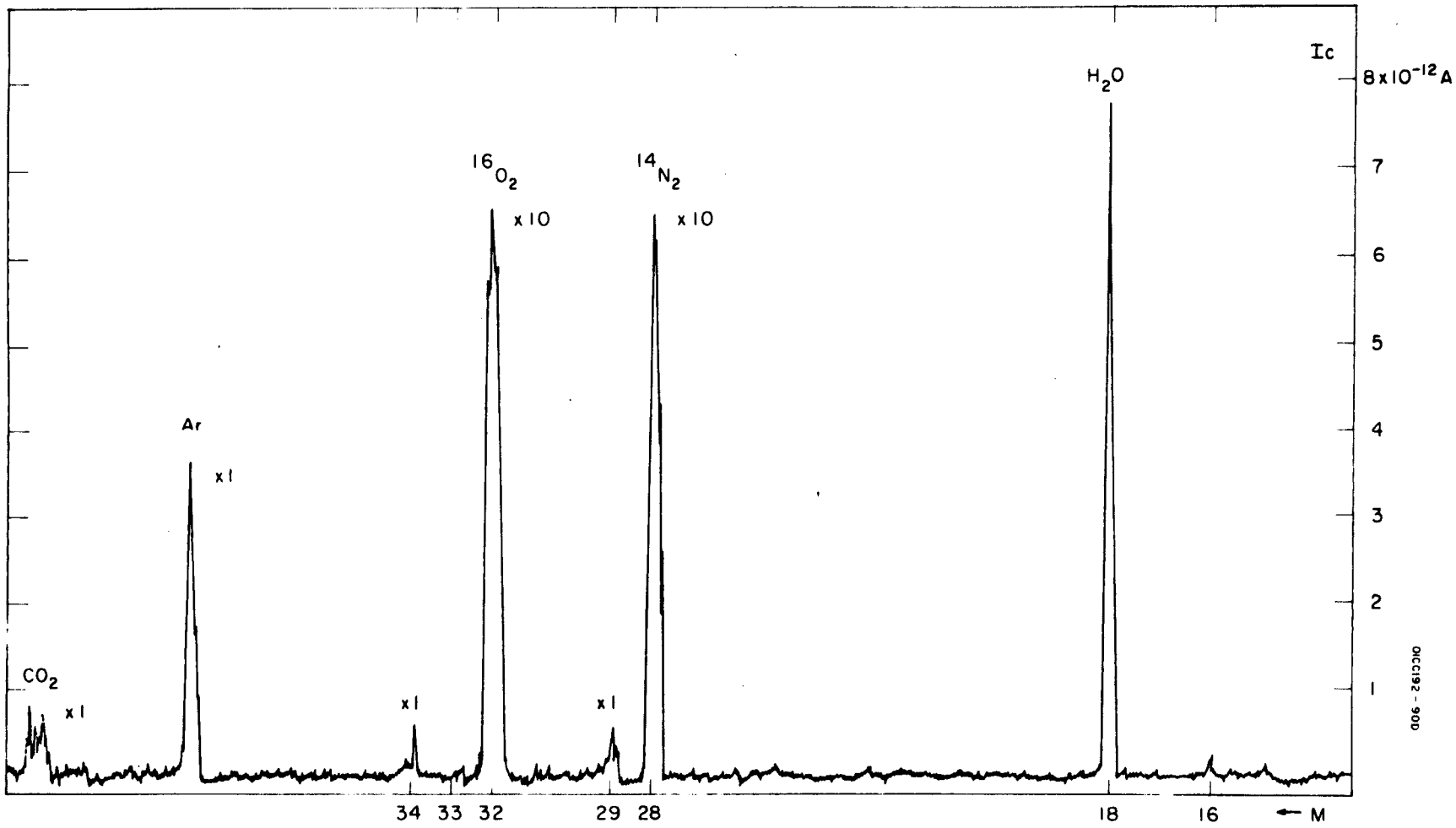

Figure 14. Background spectrum — 100 V acceleration, 788Å Ar-spark, $p_A = 6 \times 10^{-7}$ Torr, I.M.: 2300 volts.

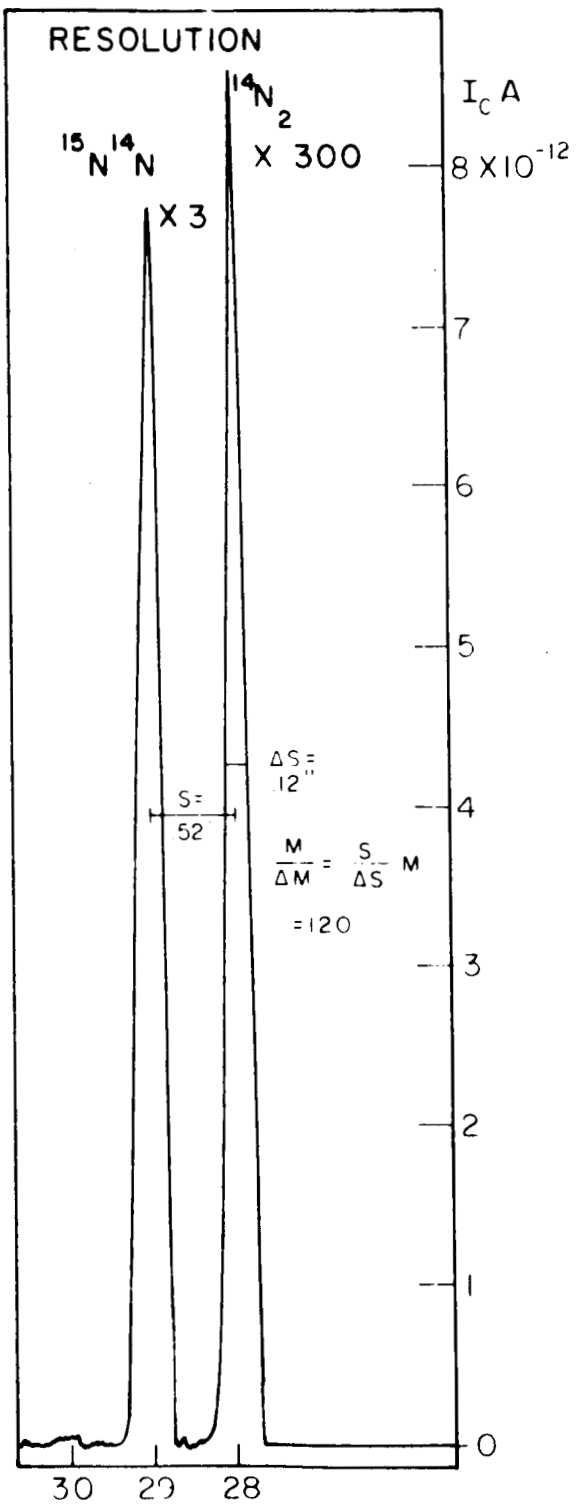

Figure 15. Demonstration of resolution.

When Figures 13 and 14 are compared, a different mass scale which is due to the different acceleration voltages used for recording both spectra can be noticed. For the correlation between mass number M, Magnet Current I_M, and Acceleration Voltage V_{acc} (voltage output at the power supply) the following formula is given:

$$M = 550 \frac{I_M^2}{V_{acc}}$$

I_M in Amps

V_{acc} in Volts

Separation of Doublets at the Same Mass Number

One of the most appealing features of photoionization lies in the possibility of utilizing the differences in the ionization potentials to discriminate between two gases occupying the same mass number. This will be demonstrated by two practical, important examples: CO in Air and CH_4 in O_2.

CO in Air. Figure 16 shows in its lowest section the uv-spectrum of the argon-spark source as obtained by scanning with the monochromator from 700 to 1000Å. The middle section gives the corresponding intensity spectrum of mass 28 with pure CO in the ion source, and the upper section the same for pure N_2 in the ion source. The X-scales for all three spectra are identical, and thus give the obvious relation between wavelength, photon intensity, and ionization efficiency for CO and N_2. The onset for CO^+ at 885Å and for N_2^+ at 796Å are easily recognized. Upon closer examination of the spectra, however, some indication of N_2^+ can be noted, also at wavelengths above the onset. Furthermore, the small peaks observed in this range do not seem to have much resemblance with the corresponding part of the uv-spectrum. This is made clearer in Figure 17 which was recorded with a higher amplification. It reveals the source of continuing ionization as being second order lines coinciding with the first order lines in this range. Those second order lines are usually not noticeably recognized in the uv-spectrum since they are obscured by the first order lines, since the sodium salicylate-photomultiplier only senses the intensities and not the energies of photons. According to the law of light dispersion on a grating, a second order line of 419Å will coincide with a first order line of twice the wavelength, i.e., 838Å. It is easily understood that any second order line falling into the first order range from 796 to 1592Å will contain sufficient energy to ionize N_2^+.

For the solution of this specific problem, a monochromatic light source with only one line between 800 and 880Å would be most ideally

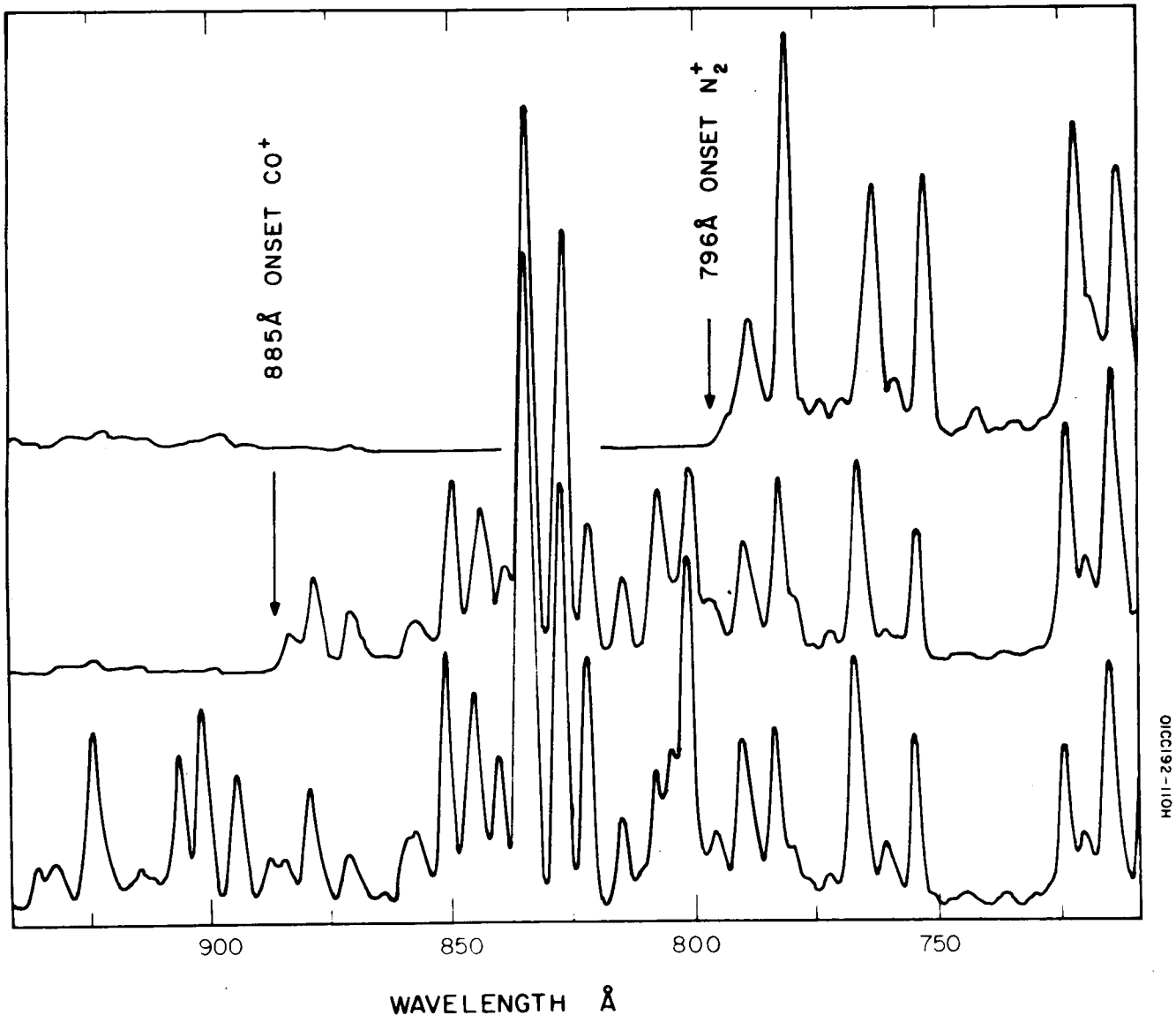

Figure 16. Spectra of N_2 and CO as a function of wavelength.

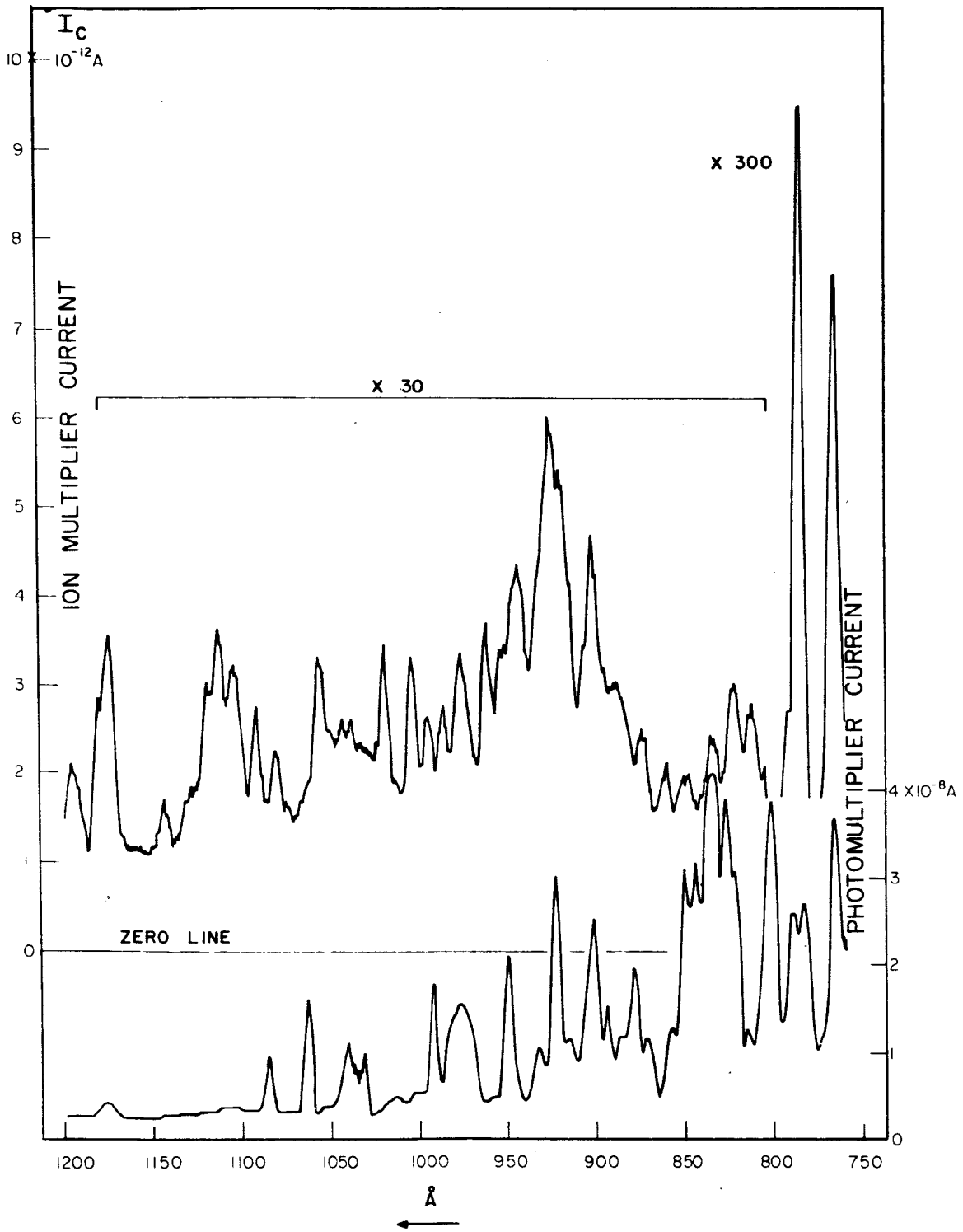

Figure 17. M = 28 peak with air ≈ 1μ Hg in ionization chamber. Argon spark source between 750 and 1200Å.

suited. Then, even the monochromator could be omitted. However, such a light source does not exist, and such an arrangement would have no flexibility for other problems. A more practical first approach seems to consist of a uv light source with a spectrum less populated at shorter wavelengths. The nitrogen spark source spectrum (Figure 11) fulfills these requirements visibly better than the argon spectrum (Figure 12). Accordingly, Figure 18 shows a tenfold reduction in the N_2^+ background signal between 796 and 1200Å. Second order peaks are considerably less pronounced, but now a continuous background becomes visible which turns out to result from light scattered in the monochromator and having a wavelength sufficient to ionize. Further attempts to reduce the remaining background signal were successful. Better baffling of the light beam in the monochromator, blackening of reflective parts close to the light beam, an additional deflection electrode to prevent electrons released at the grating from entering the ionization chamber, and better grounding resulted in a further approximately tenfold decrease of background due to scattering. The remaining background signal above 796Å on mass 28 with the exception of second order lines was then about 5×10^{-4} of N_2^+ at the strongly ionizing 765Å line.

Unfortunately, the nitrogen spark source gives only one strong line at 835Å in the range of interest between 796 and 885Å. In addition, this line gives a five times smaller ionization efficiency than N_2 at 765Å. Thus, our momentary detection limit for CO in pure N_2 lies between 0.3 percent and 0.5 percent. A further complication was found in the fact that a strong second order line with a wavelength of 419Å is in the immediate vicinity of the 835Å line and is barely resolved from the latter. Therefore, a distinctive signal on mass 28 is obtained when the 835Å peak is scanned. This signal is actually caused by ionization of N_2 through the 419Å line and is likely to mask any small contribution from CO by ionization through the 835Å line. Even more dangerous is the possibility of misinterpreting the signal as caused by CO.

Nevertheless, an unambiguous detection of 0.5 percent CO in N_2 was finally achieved. The monochromator entrance slit width was reduced until the resolution was only limited by the exit slit width, which was not changed. A resulting small intensity loss was easily overcome by a small pressure increase in the ion source. This improved the resolution to a point where the 835Å line was separated from the second order 419Å line just enough to discriminate clearly between them.

Figure 19 shows the result. The lower part gives the uv-spectrum between 760 and 850Å; the middle section the corresponding signal on the 28 peak with N_2 only; and the upper section the same with a mixture of 0.5 percent CO in N_2 admitted into the ion source. The pressure in the ion source was around 1μ. The measurement clearly shows the presence of an additional signal coinciding with the 835Å peak if CO is present. The second order 419Å peak, of course, does not show up in the uv-spectrum at this resolution since it is much smaller than the 835Å peak.

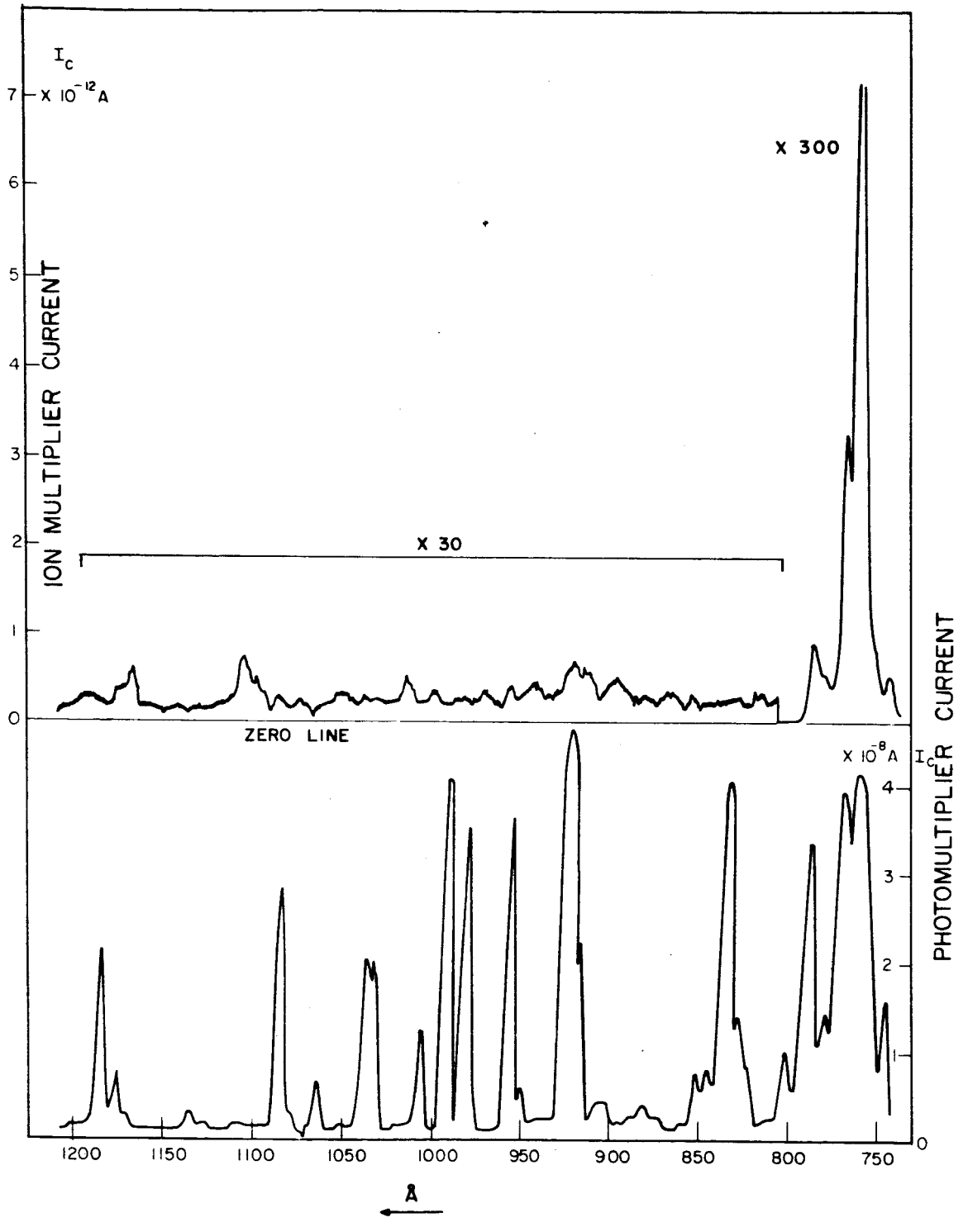

Figure 18. M = 28 peak with air ≈ 1μ Hg in ionization chamber. Nitrogen spark source between 750 and 1200Å.

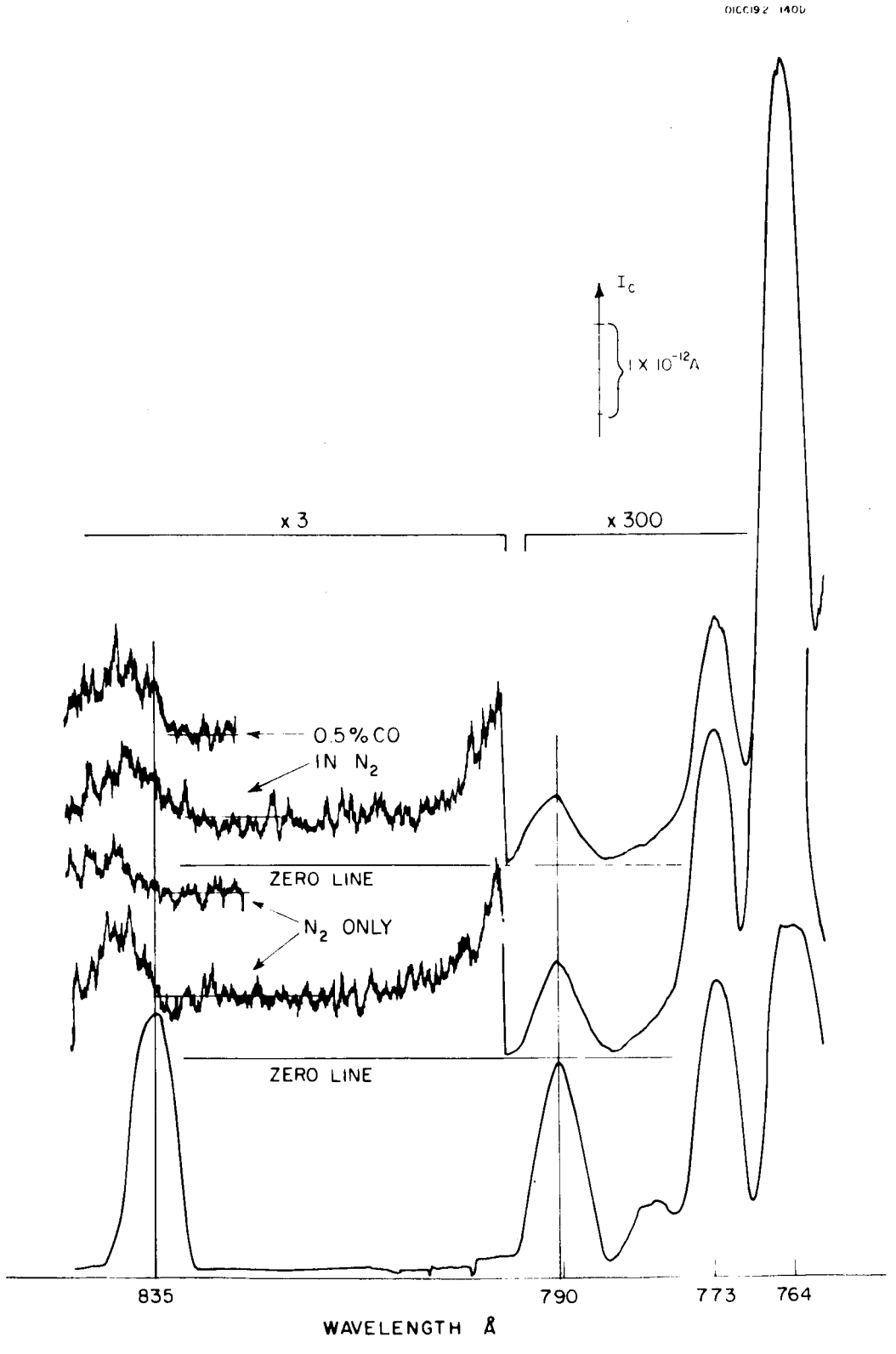

Figure 19. Detection of 0.5 percent CO in nitrogen.

The observed noise in the signal is caused by the natural statistical deviations of the ion current. The corresponding ion current on the first dynode of the multiplier is only 10^{-18} to 10^{-17} A which, with the applied integration time of the electrometer of about one second, gives a theoretical signal-to-noise ratio of less than ten.

CH_4 in O_2. Though Methane does not belong to the group of toxic gases, it gives another example of general interest showing the capability of our method. In this case, conventional electron impact ionization is limited in two ways: The high amount of oxygen is detrimental for the filament if a special Rhenium filament is not used. Second, generally a high amount, between 1 percent and 10 percent, of atomic oxygen coinciding with Methane at mass number 16 is produced. A very limited possibility to differentiate in between CH_4^+ and O^+ is given by the use of low energy electrons, but such attempts have never been too successful.

For the production of an O^+ out of O_2 an energy of 17.1 eV is required, corresponding to a wavelength of 725Å. In addition, the efficiency of this process is low, while the ionization efficiency for CH_4 is high. This presents a much more favorable condition than the detection of CO in N_2.

Figure 20 represents the analysis of a mixture of 0.14 percent CH_4 in otherwise pure O. The CH_4^+ peak corresponds to 7.2×10^{-13}A, the O_2^+ peak is 9×10^{-10}A resulting in a .125 percent ratio, close to the ratio of CH_4/O_2 in the mixture. A strong line of the nitrogen spark spectrum at 924Å (13.5 eV) was used for the ionization, and the pressure in the ion source was about 1μ Hg.

In order that the detection limit for CH_4 in O_2 might be determined, a spectrum of oxygen alone was made under exactly the same conditions. This is shown in Figure 21. Due to scattered uv light, and possibly second order interference, a small amount of atomic oxygen at M = 16 is present. The corresponding ion current is around 5×10^{-14} A - all currents measured at the output of the multiplier - and about fourteen times smaller than the signal obtained previously with CH_4. This sets the detection limit for Methane in pure oxygen at 100 ppm. The nature of small peaks at M = 15 and M = 17 in Figure 20 could not be established during this experiment. They are either random background pulses from the multiplier or may be CH_3^+ and OH^+ produced by scattered uv and second order lines. A certain evidence for those is the presence of a small N_2^+ peak.

These last recordings were made with the Keithly electrometer belonging to the mass spectrometer. The improvement achieved by better grounding can be seen from the smoothness of the zero line.

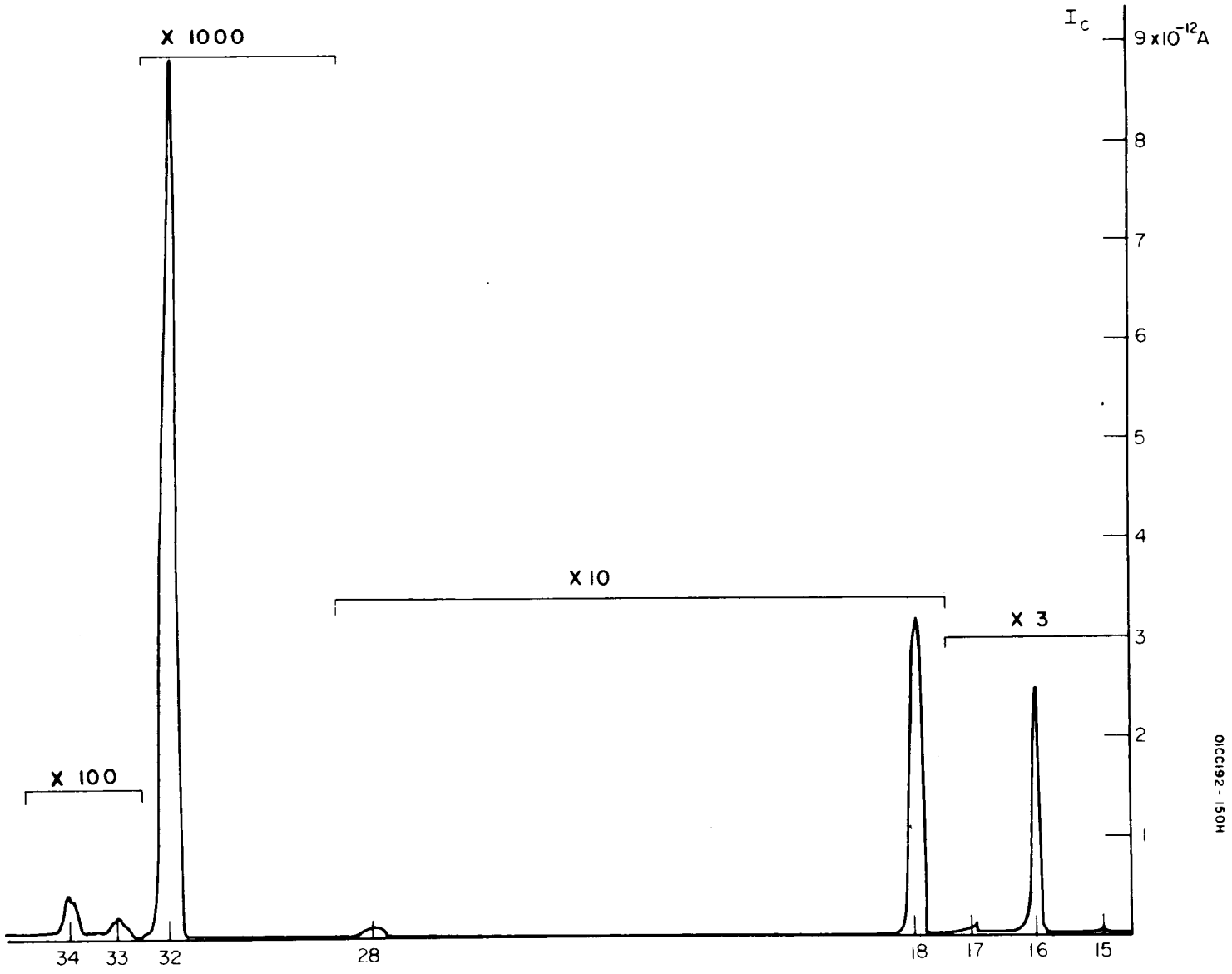

Figure 20. Spectrum of 0.145 percent CH_4 in O_2. Ionization chamber ≈ 1μ Hg. 922Å nitrogen spark, 2500 IMP, 1000 V acceleration.

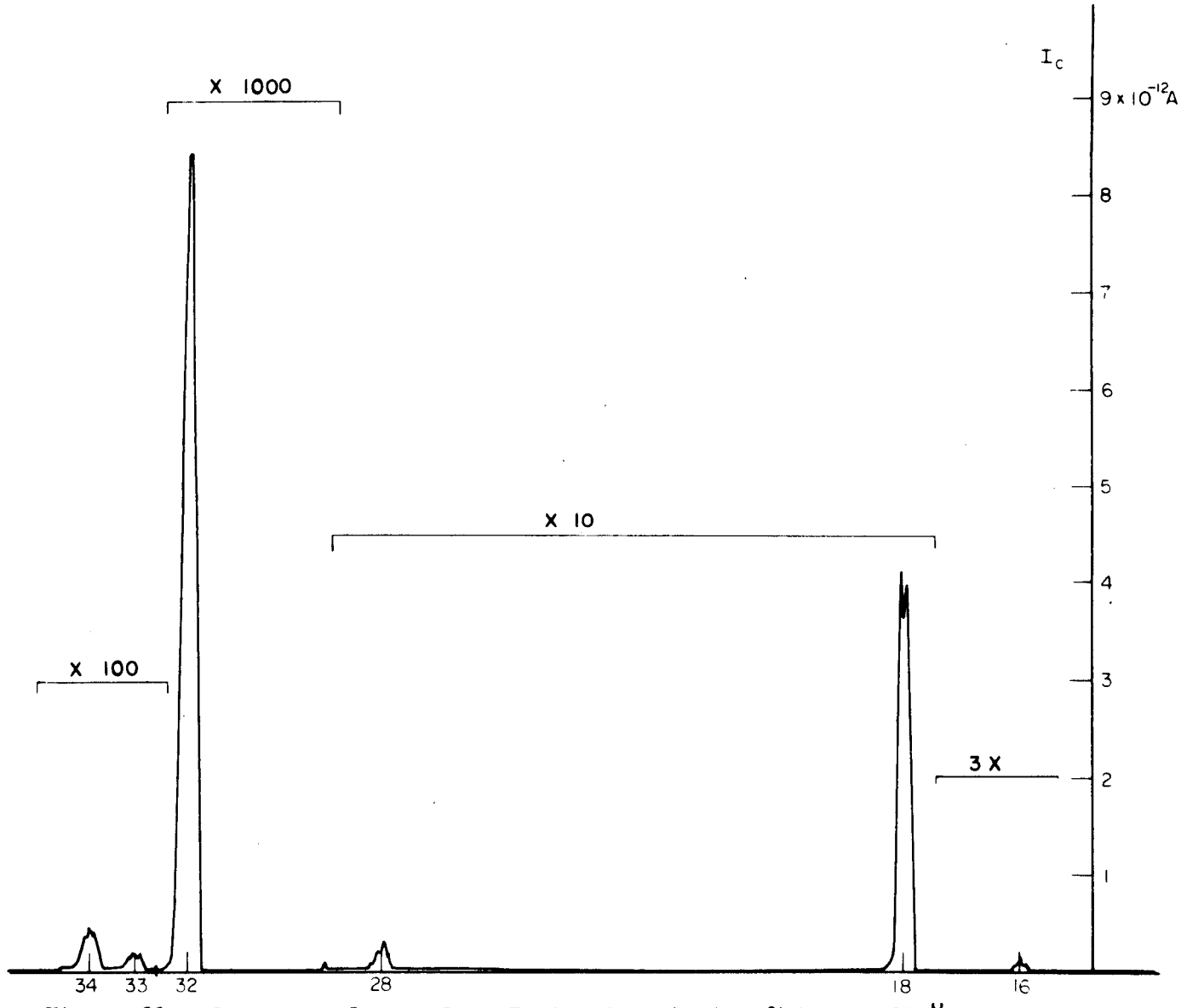

Figure 21. Spectrum of pure O_2. Ionization chamber ≈ 1μ Hg, 922Å nitrogen spark, 2500 V IMP, 1000 V acceleration.

CONCLUSIONS

The few data achieved during the limited experimental period show clearly the capability of the instrument and the feasibility of the method. Gases in a concentration between 10 ppm and 100 ppm can easily be detected by scanning. It should be mentioned that in none of the reported spectra was a gas pressure in excess of 1μ Hg used in the ion source. However, as experiments have shown, a pressure of 20μ Hg can be maintained without detriment to the performance of the instrument, yielding a twenty-fold increase in ion intensities and accordingly in sensitivity. Using lower pressures during the experiments avoided any ion molecule reactions which might happen at higher pressures. With the present monochromator, the resulting ions would not be sufficiently discriminated from ions produced by scattered uv light and second order lines. Generally, ion molecule reactions may again make spectra more complicated with higher ion source pressures. This point will need further experimental investigation.

The previous sections clearly reveal that the performance of the available monochromator imposes the most serious limitation, particularly if the separation of two ions at the same mass number is concerned. Thus, future work has to concentrate on improvements of the monochromator performance.

The monochromator had a 1200 lines/mm platinized grating which was blazed for 750Å. This has proven to be not suitable since this specific blazing particularly enhances the second order spectrum which falls into the range of interest between 800 and 900Å of the first order spectrum. A grating blazed for 1500Å will bring some improvement in the reduction of the second order.

The reduction of light scattering in the monochromator imposes some difficult problems. Avoidance of reflecting surfaces in the monochromator and careful baffling of the light beam can bring some improvement as shown in the previous sections. But a limit is soon reached when the residual scattering is mainly produced by imperfections of the grating itself. Irregularities in the line spacing of the grating will produce "ghosts". Dust particles, blisters, and similar defects in the surface of the grating will further contribute to light of uncontrolled wavelengths in the exit slit of the monochromator. With regard to the difficulties in the manufacture of such gratings, considerable improvements are hardly to be gained. At the present state-of-the-art, one might be best advised to select the best performing grating out of a larger number and then to look for another way toward a further solution of the problem.

As mentioned, second order interference and scattered light of shorter wavelengths could be avoided simply by using a light source type which produces no or only a few weak lines at wavelengths lower than needed for the ionization of the gas of interest. Thus, further work should be done to compare different uv light sources with respect to these requirements. This includes the examination of a number of different gases in the present spark source and also the utilization of different discharge types like the

conventional dc arc or the duoplasmatron [17]. The latter sources will provide somewhat smaller photon fluxes in the energy range wanted but will certainly give a sharp decrease at the unwanted higher energies. It is felt that the loss in intensity is not too serious and is compensated by the other advantages.

For the laboratory, the use of different light sources utilizing different gases will definitely improve the performance. A flight version of the instrument, however, should preferably utilize the strong uv spectrum of the sun. The sun shows an intense spectrum at wavelengths down to at least 300Å. Since in this case the source cannot be manipulated another possible solution to the problem should be investigated.

Thin metallic films of about 1000Å thickness can be used as filters on the vacuum uv range. Although the investigation of such filters is still quite recent, an increasing amount of information is already available [18-22]. From those in the group of metallic filters, an Indium filter seems to be most suitable for our purpose. It has good transmittance between 750 and 1000Å with a sharp cutoff below 750Å which reaches down to about 100Å (Figure 22).

Another alternative consists of the use of a gas filter, which takes advantage of the absorption properties of atoms and molecules to provide selective filtering. Of particular use are filters of rare gases. These gases are essentially transparent to wavelengths longer than their ionization potential; however, to shorter wavelengths, they are strongly absorbing. Thus, with the use of an absorption cell of 20 cm length filled with argon at a pressure ~ 500μ, no radiation between 300 and 787Å will be transmitted [22]. The spectrum will, therefore, be free from second order lines from 878 to 1474Å. Equally all scattered light with wavelengths between 300 and 787Å will be eliminated.

Regarding all the data available, it is believed that by such efforts the discriminating power of the instrument can be considerably increased. The present detection limit of 0.5 percent CO in air might be extended to and even beyond 100 ppm. Some intensity loss will be encountered by filtering but should be overcome by the reserves still given in the ion source pressure. If necessary, a further increase in sensitivity can be gained if a pulse counting technique with pulse height discrimination is applied instead of electrometric recording. This results in a reduction in the random background signals from the multiplier of up to one order of magnitude [23], and in any case, should suffice to maintain the general detection limit of the instrument in the range of parts per million.

Finally, we may say that the instrument and the results described here already clearly prove the feasibility of our approach to analyze the atmosphere in a spacecraft. The photoionization mass spectrometer can reach sensitivities equal to conventional mass spectrometers but has unsurpassed additional capabilities. Since its use is not limited to gas analysis, it is a valuable instrument for research in the field of photoionization, photodissociation, and ion molecule reactions.

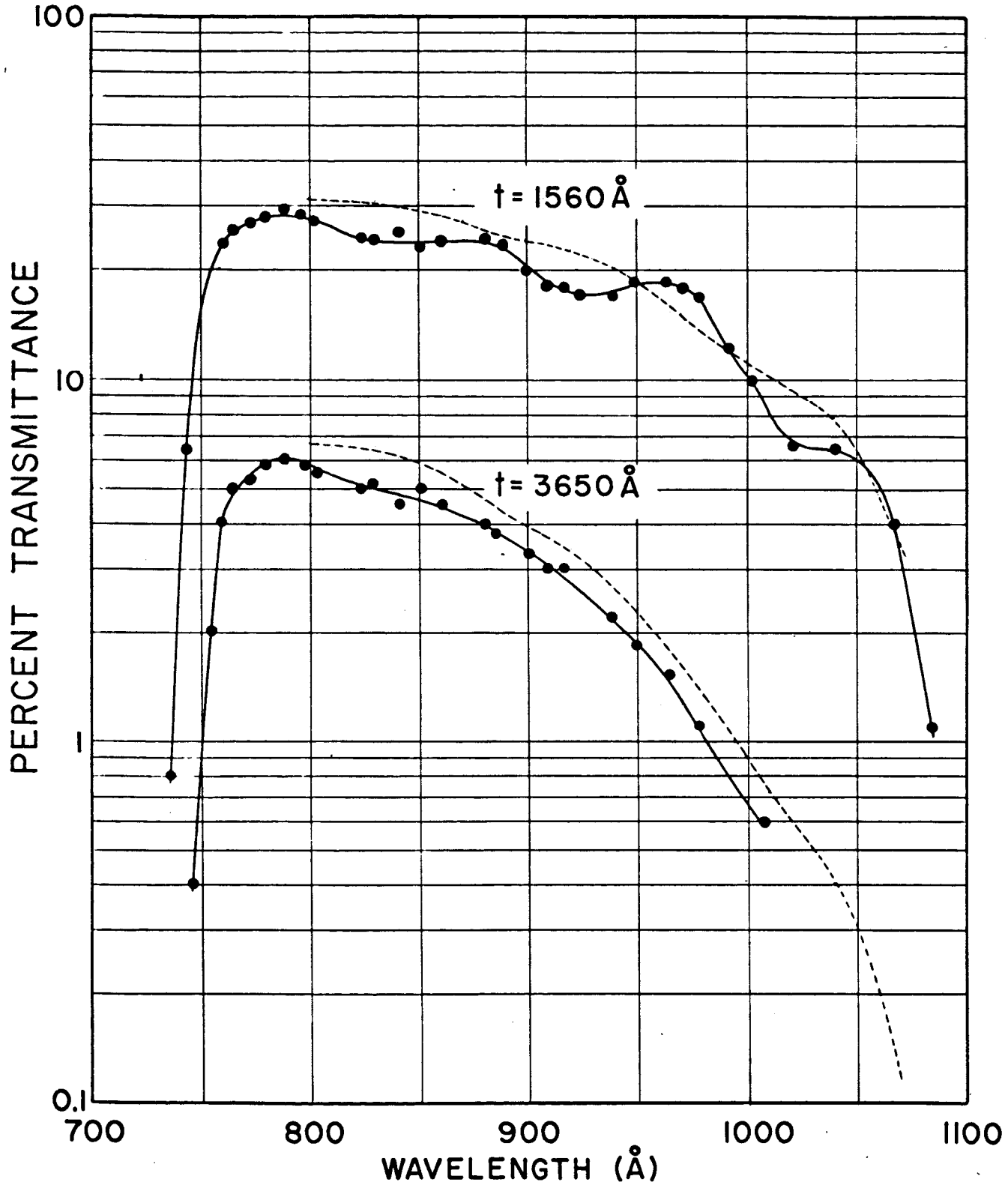

Figure 22. Transmittance of indium films. Dashed lines are calculated values.

APPENDIX

THE FEASIBILITY OF A FLIGHT INSTRUMENT

Though the photoionization mass spectrometer seems in principle to be quite applicable for the analysis of the atmosphere in a space capsule, the size, weight, and power consumption of the laboratory instrument seem to be a very discouraging factor. However, this consideration is misleading for the following reasons:

Much of the weight and size of the instrument is contained in the vacuum system, which can be omitted in space application. At an altitude beyond 100 km, the pressure of the earth's atmosphere is less than 10^{-4} torr. Since no vacuum pumps are needed, the power requirements are considerably reduced.

Instead of the artificial uv light source with its bulky power supply and cooling requirements, the natural uv spectrum of the sun can be used. Figure 23 shows the continuum of the sun between 100 and 1000Å and Figure 24 shows the spectral emission lines superimposed onto this continuum. The photon flux of the continuum is given in number of photons per sec per cm^2 and per 50Å. Thus, if only a resolution of the order of 50Å is required, the continuum contributes equal or more to ionization than do the discrete lines. This can be used to compensate for the generally smaller photon flux in the uv region if compared with the spark source. A further possibility for an increase in the photon flux consists in the use of a solar collector. Some metallic mirrors provide reasonable reflectivity at the considered wavelengths. The construction of such a collector system with an attached monochromator will require further special efforts but can certainly be realized. Should the solar collector concept fail, however, the development of a special uv light source is still possible.

It also appears feasible to eliminate the heavy magnetic laboratory mass spectrometer and use a lightweight high frequency mass spectrometer such as the successful quadrupole or monopole type.

At this point, however, it is not too meaningful to go into too many details. The laboratory instrument used in ground tests first has to yield more detailed results concerning the actual consistency of the atmosphere in a spacecraft. On the basis of these results, the most economical final approach can be conceived toward a flight instrument.

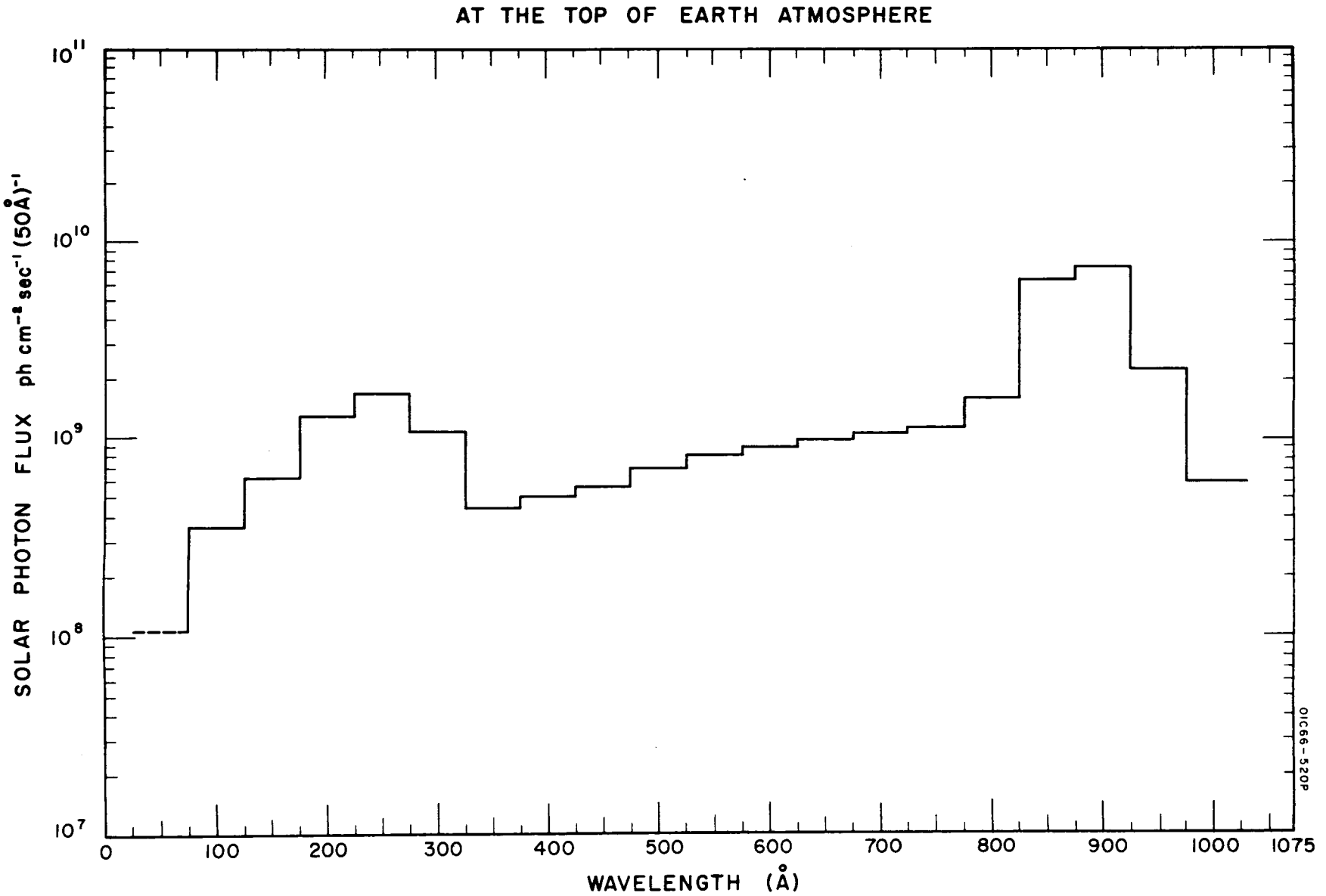

Figure 23. Solar photon flux — continuum to 1000Å.

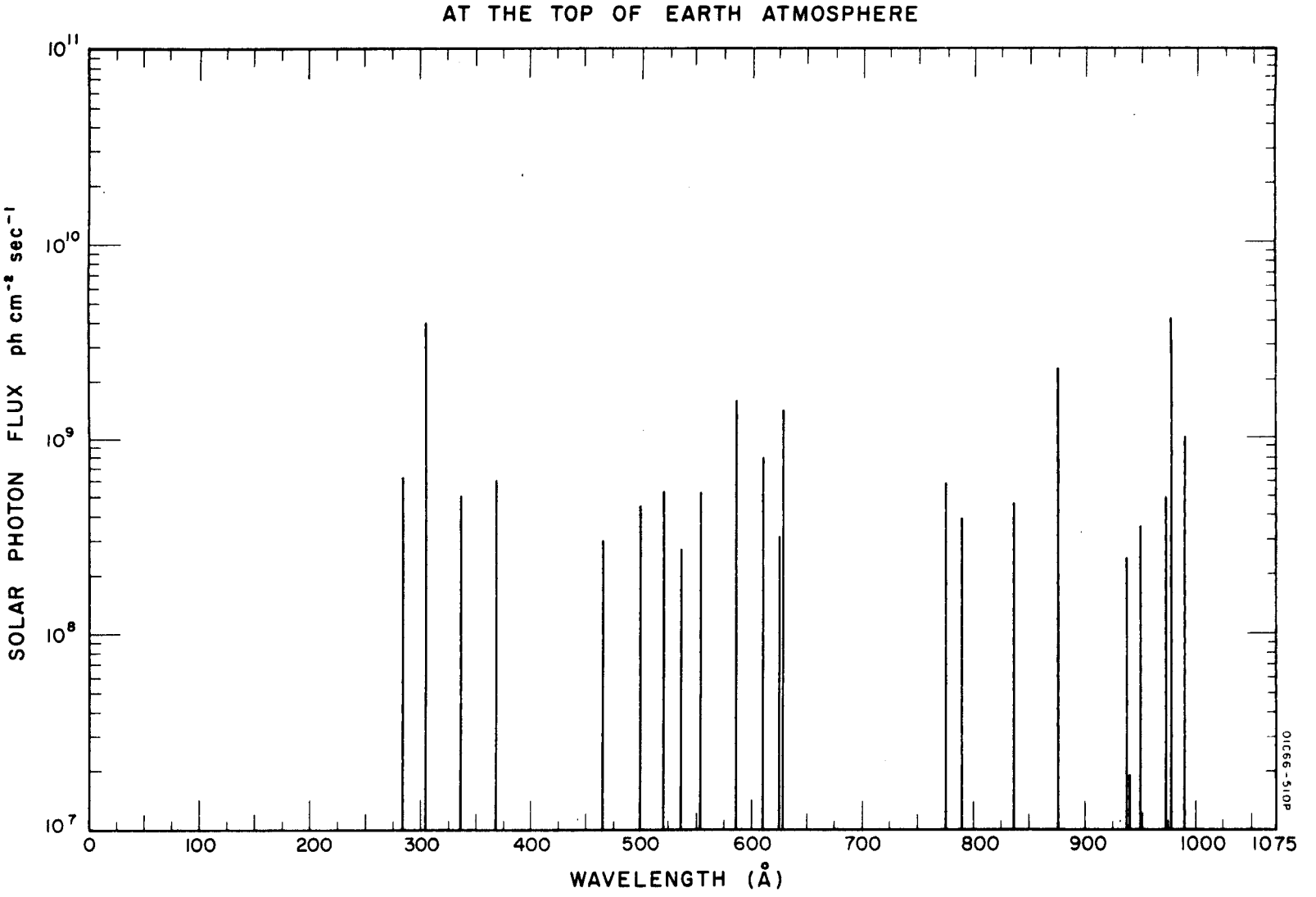

Figure 24. Solar Photon flux – emission lines to 1000Å.

REFERENCES

1. Ahearn, A. J., Mass Spectrographic Studies of Impurities of Surfaces, 1959 Sixth National Symposium on Vacuum Technology Transactions, 1-5, Pergamon Press, Inc., New York (1960).

2. Handbook of Chemistry and Physics, Published by the Chemical Rubber Co., Cleveland, Ohio, 46th Edition, p. F49.

3. Sax, N. I., Dangerous Properties of Industrial Materials, Reinhold Publishing Corp., New York.

4. Elder, F. A., Giese, C., Steiner, B. and Inghram, M., "Photoionization of Alkyl Free Radicals," J. Chem. Phys. 36, 3293-3296 (1962).

5. Steiner, B., Giese, C. and Inghram, M., "Photoionization of Alkanes; Dissociation of Excited Molecular Ions," J. Chem. Phys. 34, 189-220 (1961).

6. Schoen, R. I., "Absorption, Ionization, and Ion Fragmentation Cross Sections of Hydrocarbon Vapors under Vacuum - Ultraviolet Radiation," J. Chem. Phys. 37, 2032-2040 (1962).

7. Hurzeler, H., Inghram, M. and Morrison, J. P., "Photon Impact Studies of Molecules using a Mass Spectrometer," J. Chem. Phys. 28, 76-82 (1958).

8. Dibeler, V.H. and Reese, R. M., "Mass Spectrometric Study of Photoionization..," J. Res. Natl. Bur. Std. 68a, 409 (1964).

9. Comes and Lessmann, W., "Ionenbilding im Stickstoff," Z. Naturforschung, 19a, 65 (1964).

10. Jensen, C. A. and Libby, W. F., "Intense 584Å - Light from a Simple Continuous Helium Plasma," Phys. Rev. 135A, 1247 (1964).

11. Richardson, H. O. W., "Magnetic Focussing between Inclined Plane Pole-Faces," Phys. Soc. Proc. (London) 59, 791 (1947).

12. Connell, J. S., "Simple Broad Range Magnetic Spectrometer," Rev. Sci. Instr. 32, 1314 (1961).

13. Herzog, R. F. K., Z. Physik 97, 596 (1935).

14. Samson, J. A. R., "Absolute Intensities in the Vacuum Ultraviolet," J. Opt. Soc. Am. 54, 6 (1964).

15. Lampe, F. W., Franklin, J. L. and Field, F. H., Progress in Reaction Kinetics, Vol. 1, ed. C. Porter, Pergamon Press, p. 69 (1961).

16. Weissler, G. L., Samson, J. A. R. and Cook, G. R., "Photoionization Analysis by Mass Spectroscopy," J. Opt. Soc. Am. 49, 338-349 (1959).

17. Samson, J. A. R. and Liebl, H. J., "Duoplasmatron as a Vacuum Light Source," Rev. Sci. Instr. 33, 1340-1343 (1962).

18. Hunter, W. R., Angel, D. W. and Tousey, R., "Thin Films and Their Uses for the Extreme Ultraviolet," Appl. Optics 4, 891 (1965).

19. Townsend, J. R., "Solid-State Absorption Spectra of Mg and MgO," Phys. Rev. 92, 556 (1953).

20. Walker, W. C., "d-Band Transitions in Solids," J. Phys. Chem. Solids 24, 1667 (1963).

21. Rustgi, O. P., "Transmittance of Thin Metallic Films in the Vacuum Ultraviolet Region Below 1000Å," J. Opt. Soc. Am. 55, 630 (1965).

22. An extensive discussion of the present state-of-the-art of uv filters will be found in Chapter VI of: Samson, J. A. R., Techniques of Vacuum Ultraviolet Spectroscopy, John Wiley and Sons, New York, to be published about September 1966.

23. Kendall, B. R. F., "Electron Multipliers for Use in Mass Spectrometry," Nuclide Contribution 64-03, Presented at Annual Meeting of A.S.T.M., E-14 at Montreal (June 1964).

SELECTED BIBLIOGRAPHY

(Not specifically referred to in the report but of pertinent interest)

Lossing, I.P. and Tanake, I., "Photoionization as a Source of Ions for Mass Spectrometry," J. Chem. Phys. 25, 1031 (1956).

Herzog, R. F. K. and Marmo, F. F., "Mass Spectroscopic Determination of Photoionization Products," J. Chem. Phys. 27, 1202 (1957).

Boion, C. E., "A Windowless Photoionization Source for High Resolution Analytical Mass Spectrometers," Analyt. Chem. 37, 1707 (1965).

Schönheit, E., "Massenspektrometrische Untersuchung der Photoionisation von Wasserstoff," Z. Naturforschung 15a, 841 (1960).

Dibeler, V. H., Reese, R. M. and Krauss, M., "Mass Spectrometric Study of Photoionization II, H_2, HD, and D_2," J. Chem. Phys. 42, 2045 (1965).

Dibeler, V. H., Krauss, M., Reese, M. and Harllee, F., "Mass Spectrometric Study of Photoionization III, Methane and Methane-d_4," J. Chem. Phys. 42, 3791 (1965).